



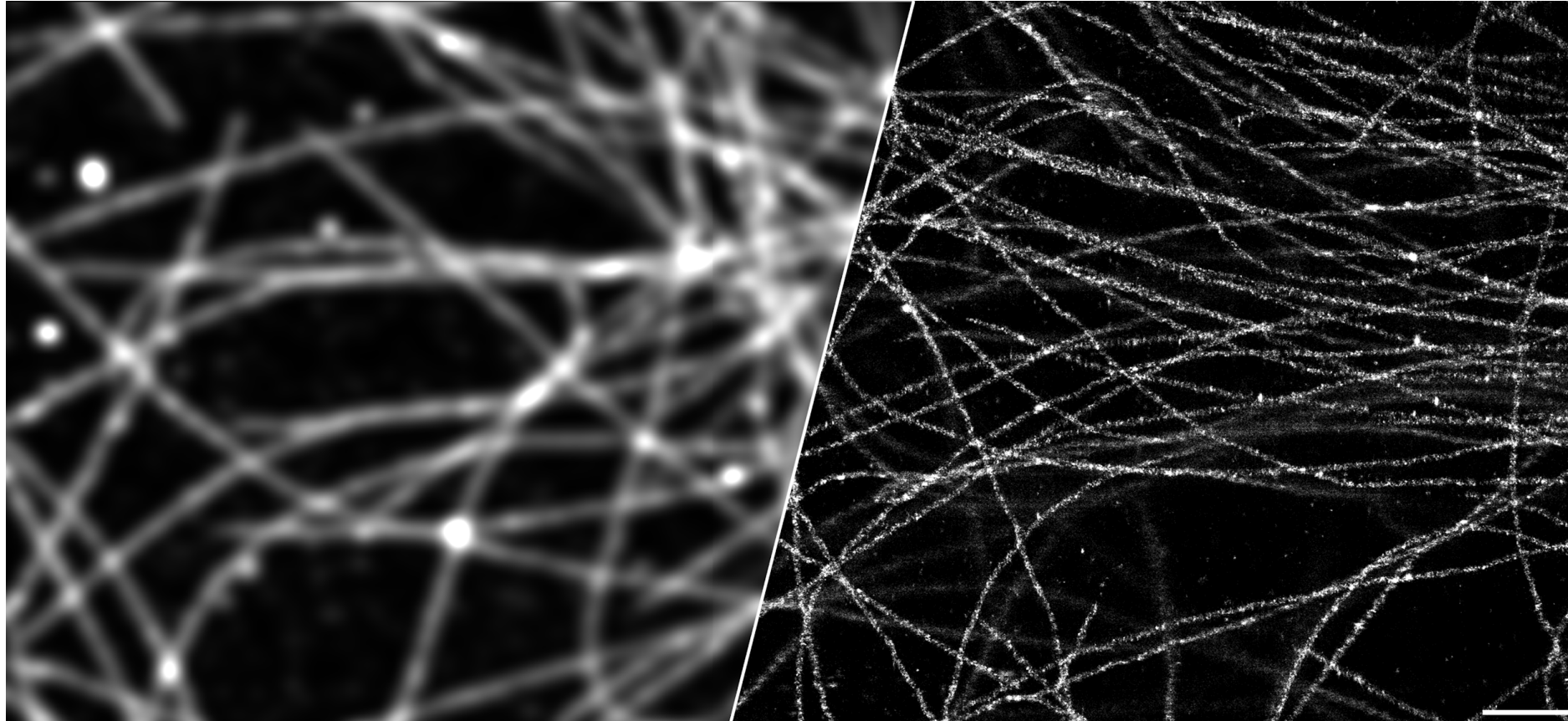
Single-Molecule Localization Microscopy: Theoretical Basis and Practical Guide

“Widening the Lens” Microscopy Education program
Vanderbilt University, Nashville, TN, USA

Ulrike Boehm, Ph.D.

ulrike.boehm@zeiss.com - @ulrike_boehm
Corporate Research & Technology (CRT), Carl Zeiss AG

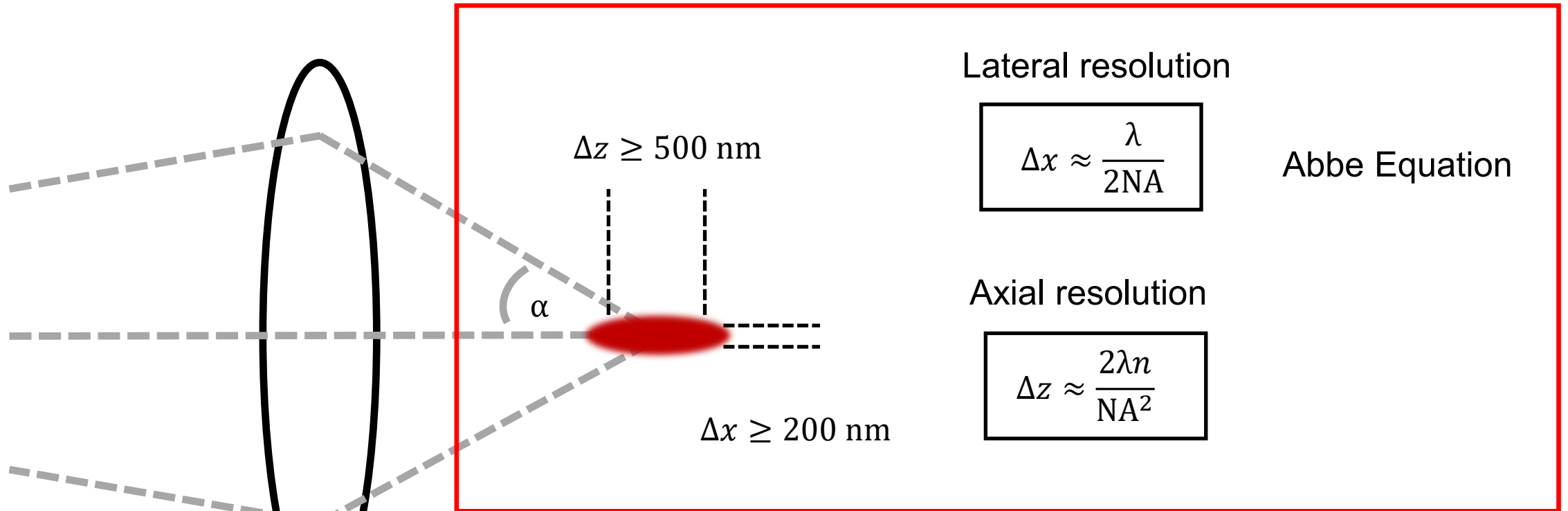
Diffraction Limited vs. Diffraction **Un**limited



Microtubules, scale bar: 1 μm

The Diffraction Limit

Point Spread Function (PSF)



λ – wavelength

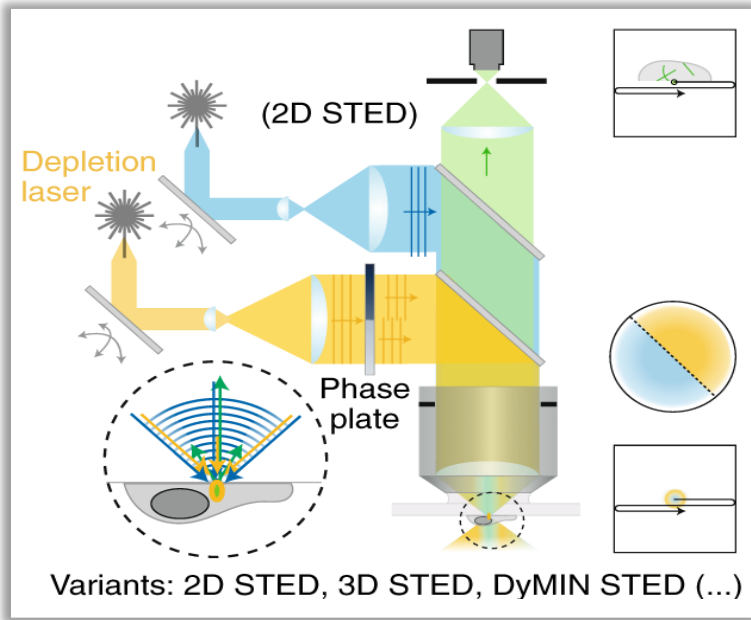
α – semi aperture angle

n – refractive index

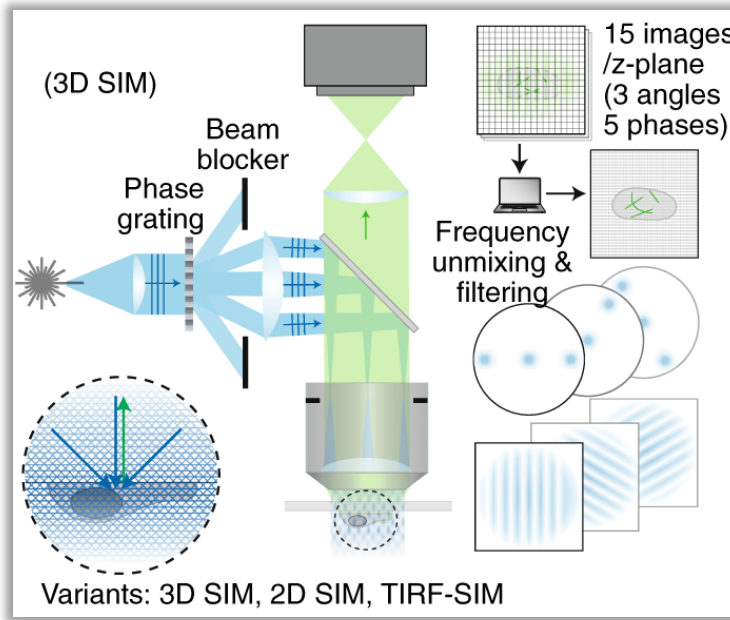
NA – refractive index

$$NA = n \sin \alpha$$

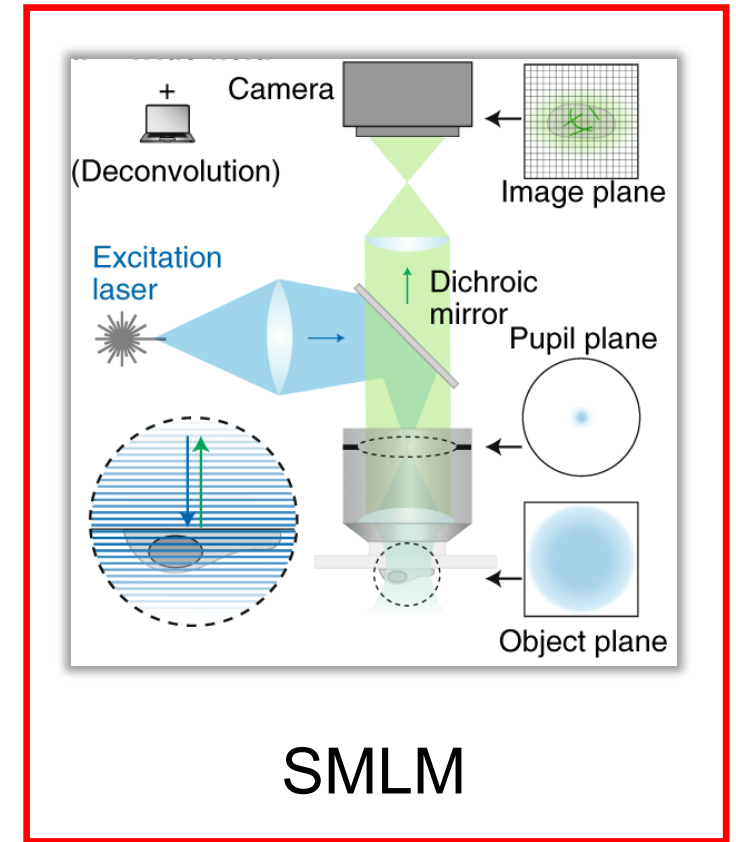
Circumventing the diffraction limit with...



STED



SIM

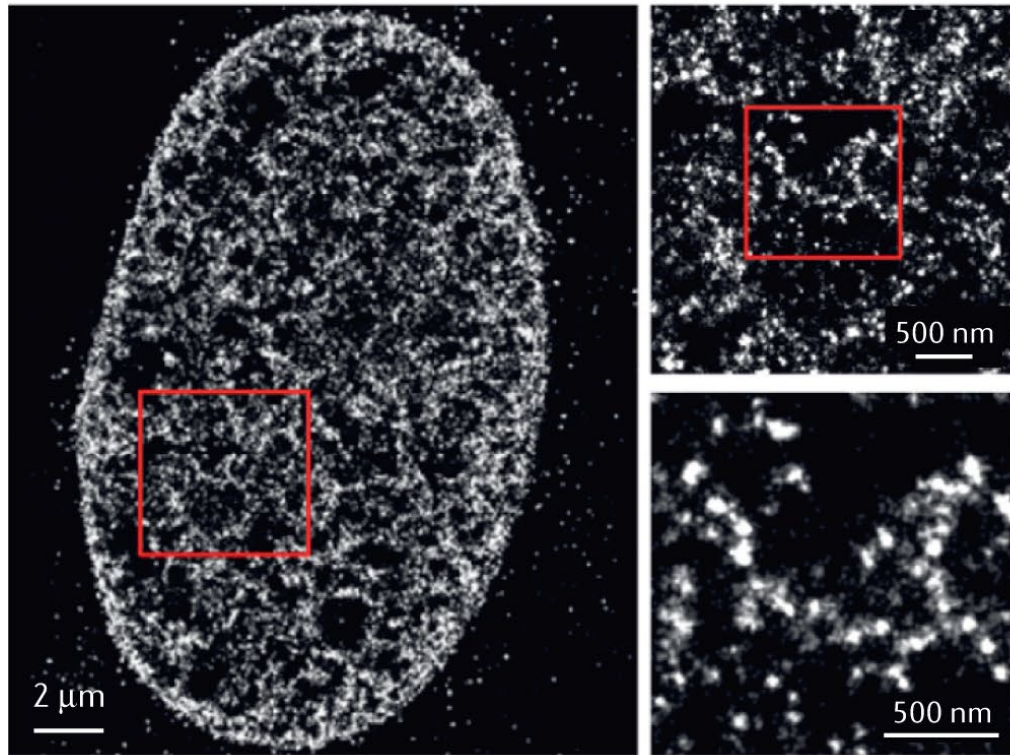


SMLM

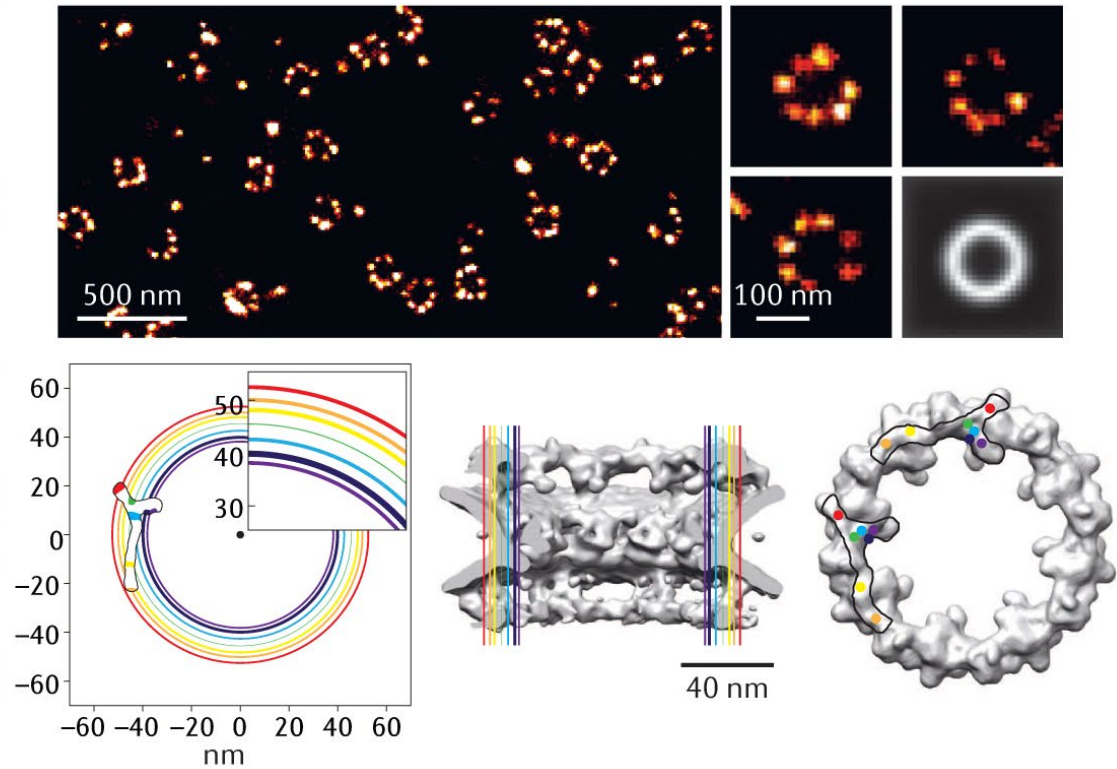
This lecture's focus

Major discoveries enabled by SMLM

a Nucleosome clutches

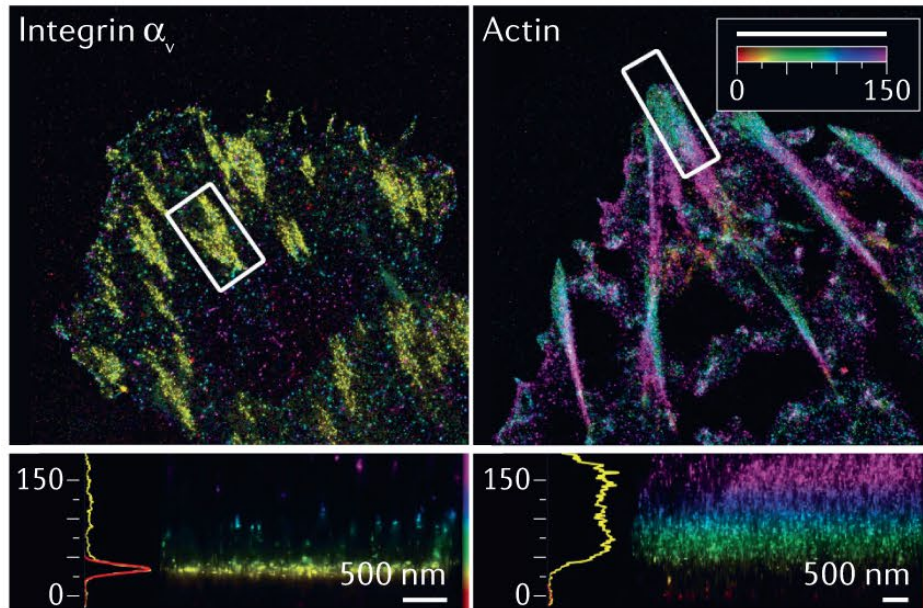


b Nuclear pore complexes

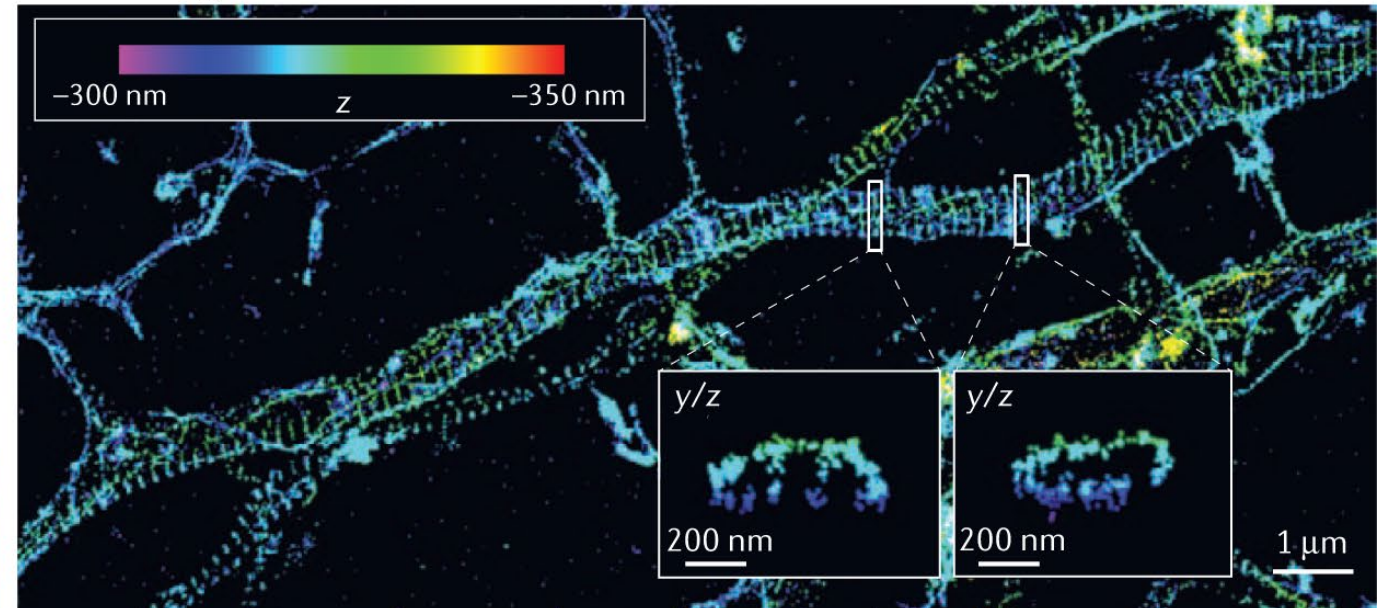


Major discoveries enabled by SMLM

c Focal adhesion nanoarchitecture



d Actin rings



Overview

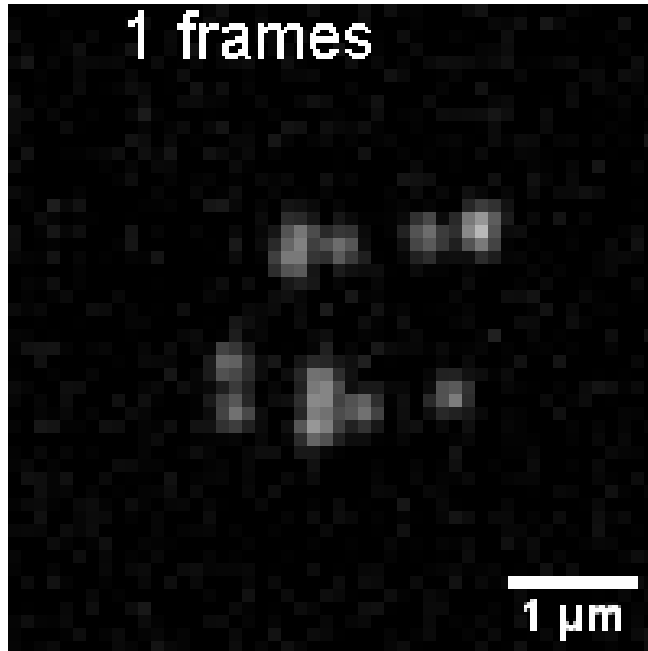
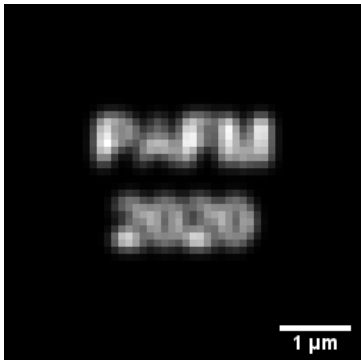
- Basic principles 2D SMLM
- Hardware for SMLM
- Practical considerations: sample preparation, suitable dyes, linkage errors, and buffers
- Processing, quantification, and interpretation of SMLM data
- 3D SMLM
- Summary

- Extra: New directions in SMLM
- Extra: SRM as a multidimensional challenge

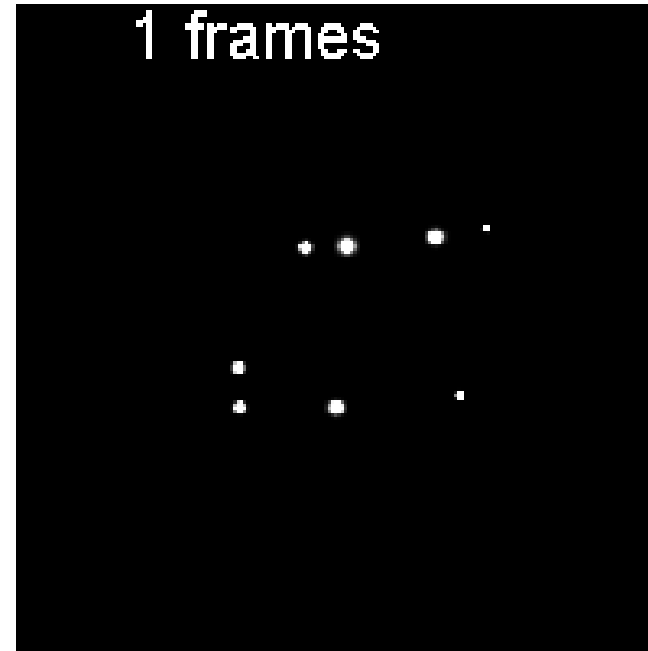
Basic principles of 2D SMLM

What is Single Molecule Localization Microscopy (SMLM)?

Widefield image



Sequence of widefield images



Accumulated localizations

Superresolution image



What is Single Molecule Localization Microscopy (SMLM)?

Sample Preparation

Processing

Superresolution image

Widefield image

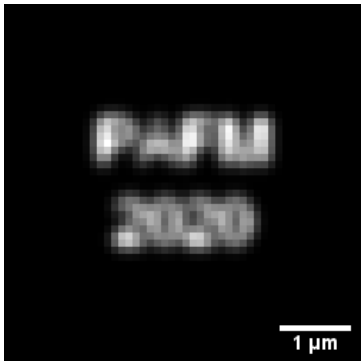


Image Acquisition

1 frames

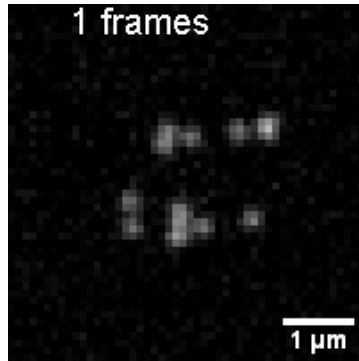


Image at t_1

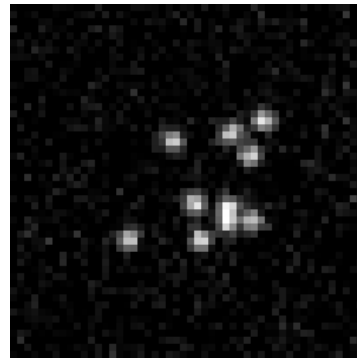


Image at t_2

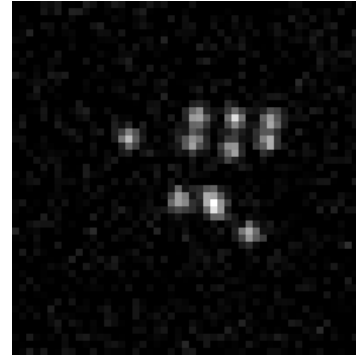
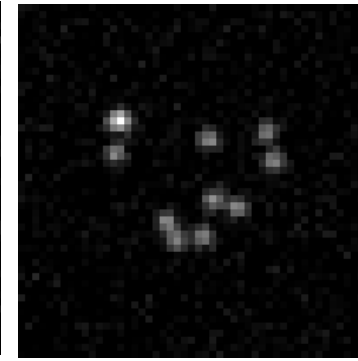
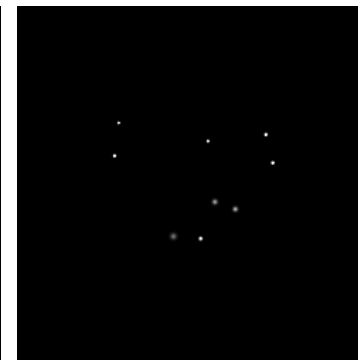
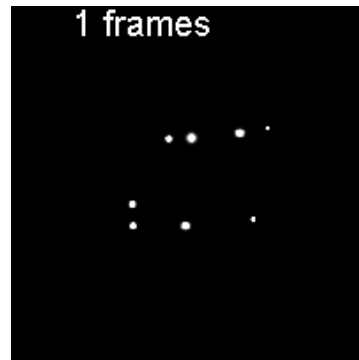


Image at t_3



Hardware

1 frames




$$t_1 < t_2 < t_3$$

What is Single Molecule Localization Microscopy (SMLM)?

- In SMLM small subsets of individual emitters are randomly activated or switched ON/OFF in consecutive acquisitions.
- If sparse enough to be identified as single molecule switching events, signals become spatiotemporally separated and are collected over several thousands of camera frames.
- Raw data are computationally processed to detect single molecules and determine their center positions with nanometer precision dependent on the number of photons detected per individual emitter.
- These are finally assembled through superimposition into a single-plane image.

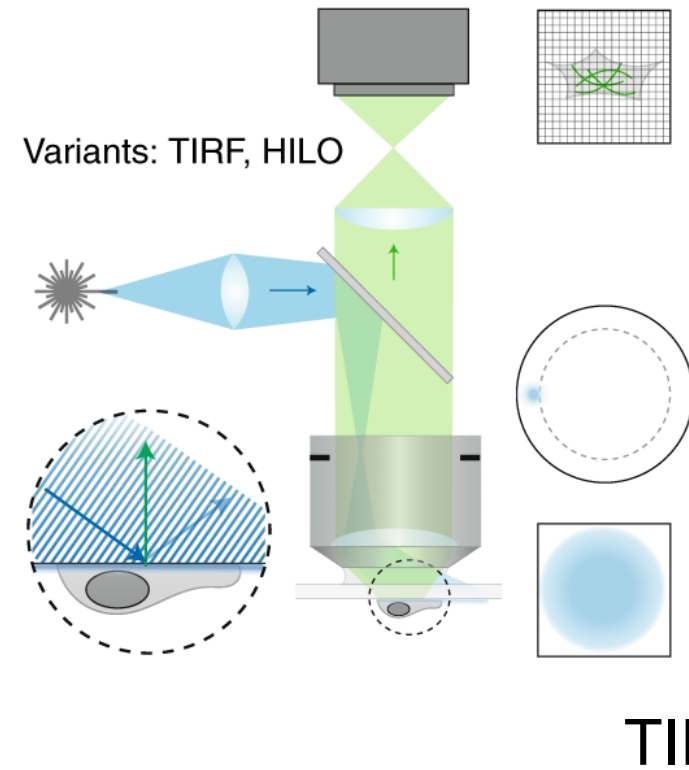
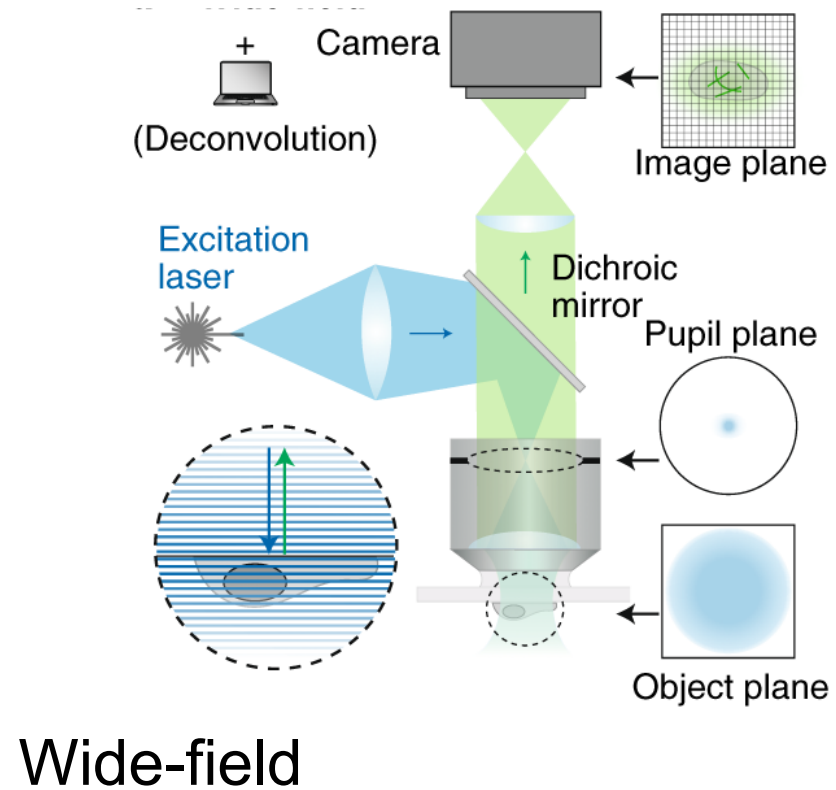
Overview

- Basic principles 2D SMLM 
- Hardware for SMLM
- Practical considerations: sample preparation, suitable dyes, and buffers
- Processing, quantification, and interpretation of SMLM data
- 3D SMLM
- Summary

- Extra: New directions in SMLM
- Extra: SRM as a multidimensional challenge

Hardware for SMLM

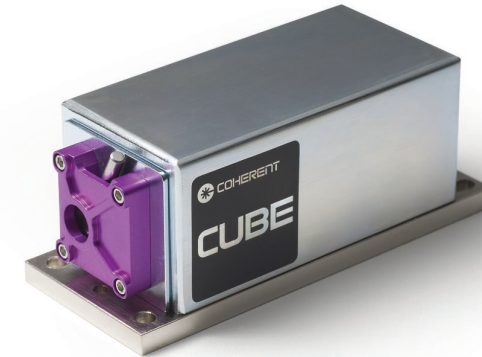
Hardware for SMLM



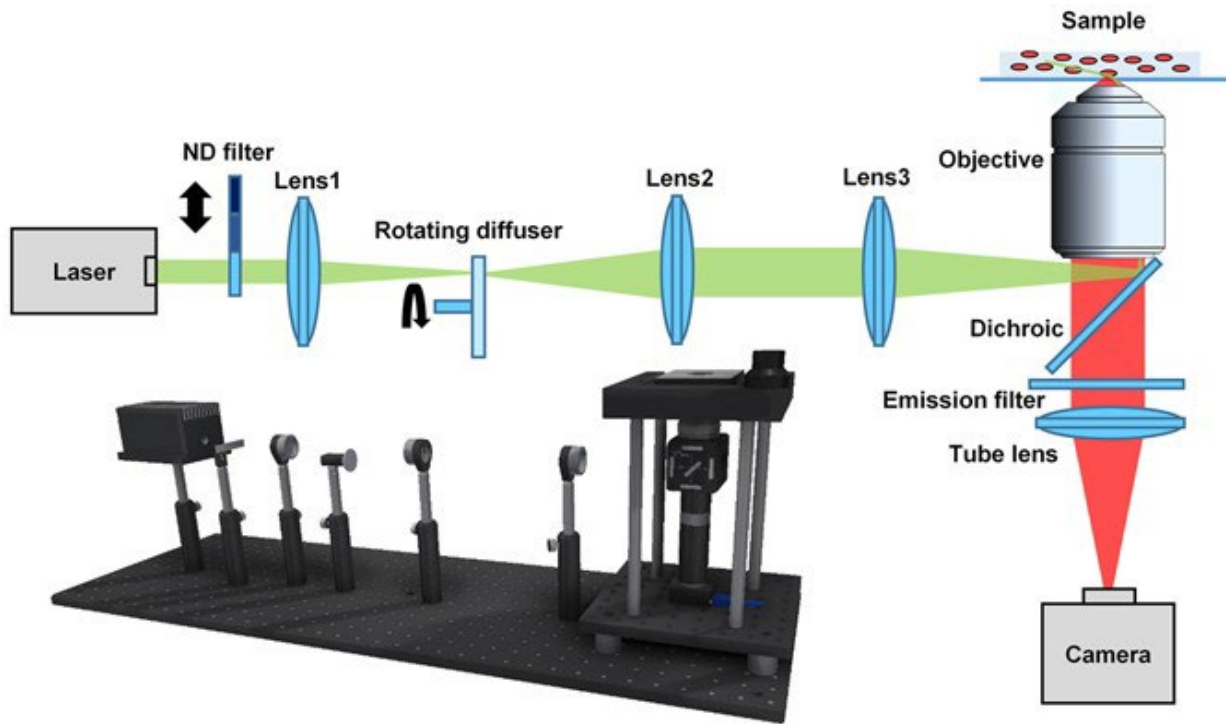
Hardware for SMLM

- Wide-field or TIRF with high NA objectives (15k-20k)
- High power lasers (~25k)
- Sensitive EMCCD (~35k) or sCMOS (~16k) cameras
- Additional optics for 3D information

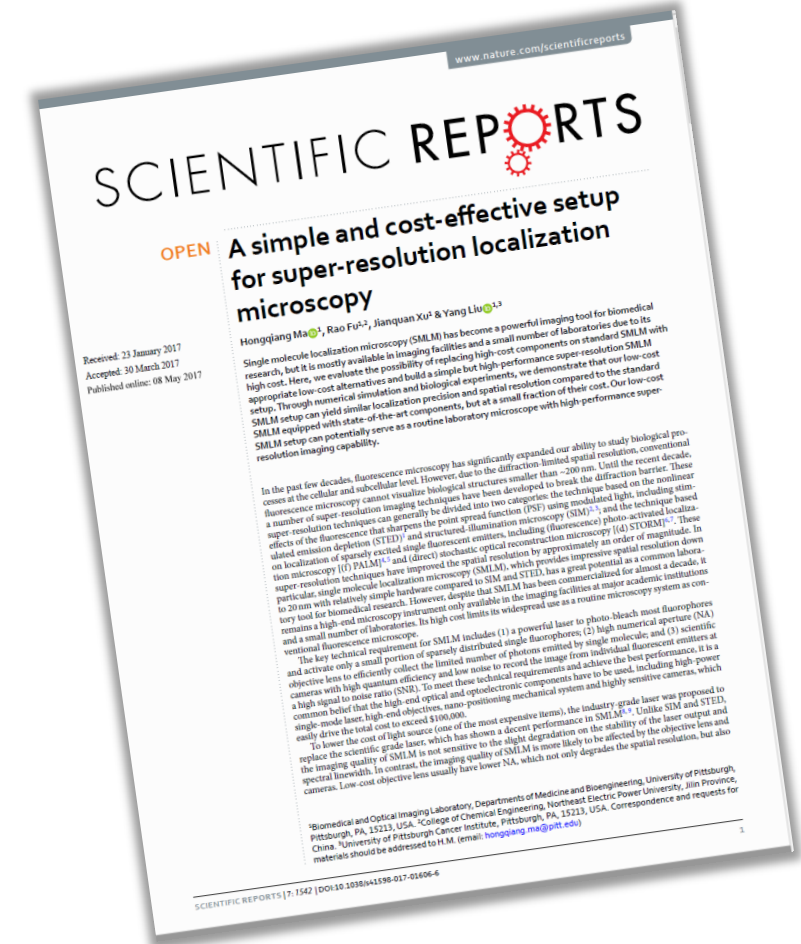
System upgrade:
~\$80,000





Hardware for SMLM



Total cost: \$4,100.00



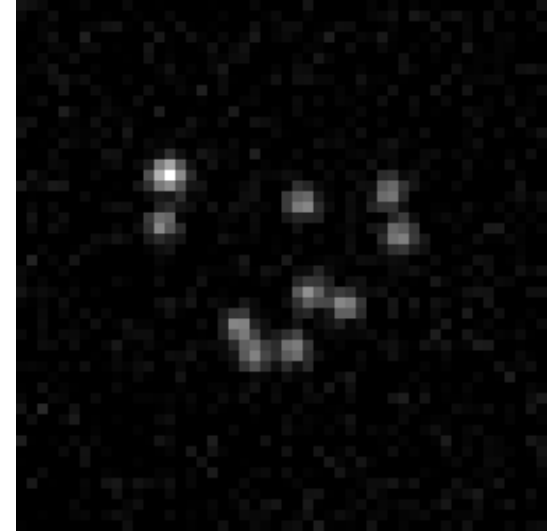
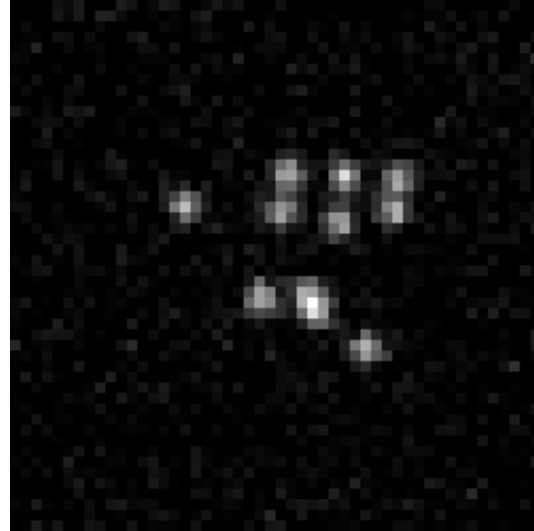
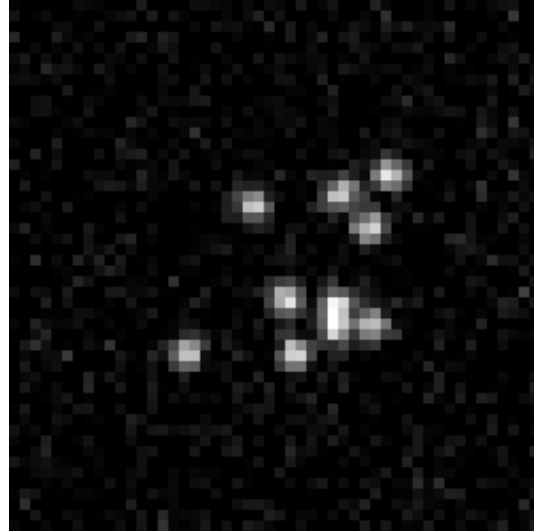
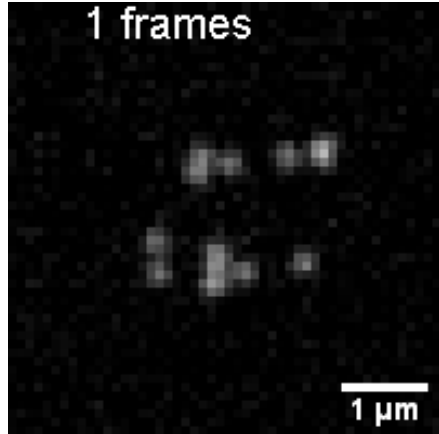
Overview

- Basic principles 2D SMLM 
- Hardware for SMLM 
- Practical considerations: sample preparation, suitable dyes, linkage errors, and buffers
- Processing, quantification, and interpretation of SMLM data
- 3D SMLM
- Summary

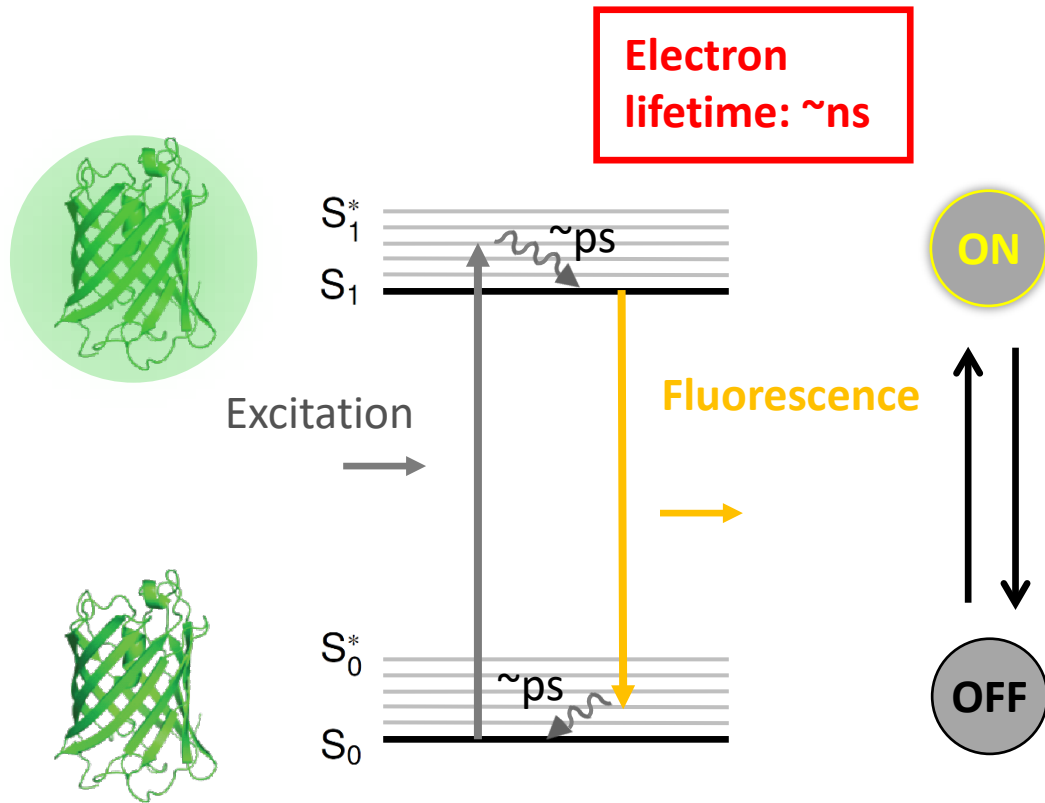
- Extra: New directions in SMLM
- Extra: SRM as a multidimensional challenge

**Practical considerations: sample preparation,
suitable dyes, linkage errors, and buffers**

Photoswitching – ON/OFF switching

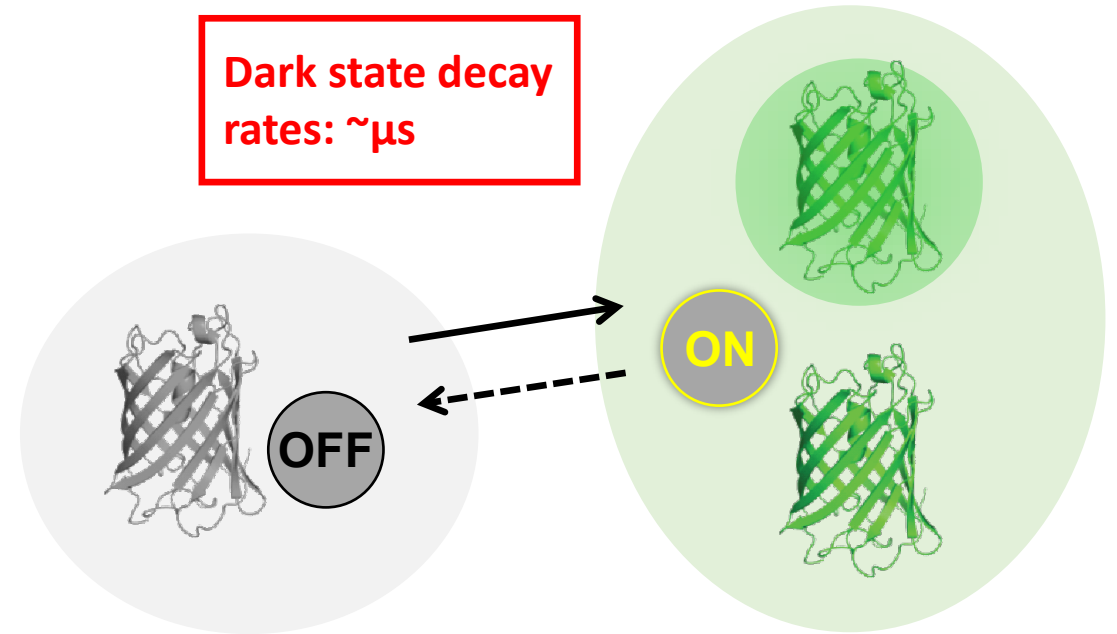


Photoswitching – ON/OFF switching



Conventional dyes

Temporal separation not possible



Typical SMLM dyes

“Dark” state allows temporal separation for SMLM

A good SMLM dye has...

Long ON-time to allow the collection of many photons, but not too long such that the data acquisition is slowed down.

Complete dark OFF-state that is long enough to prevent too many fluorophores from being ON simultaneously.

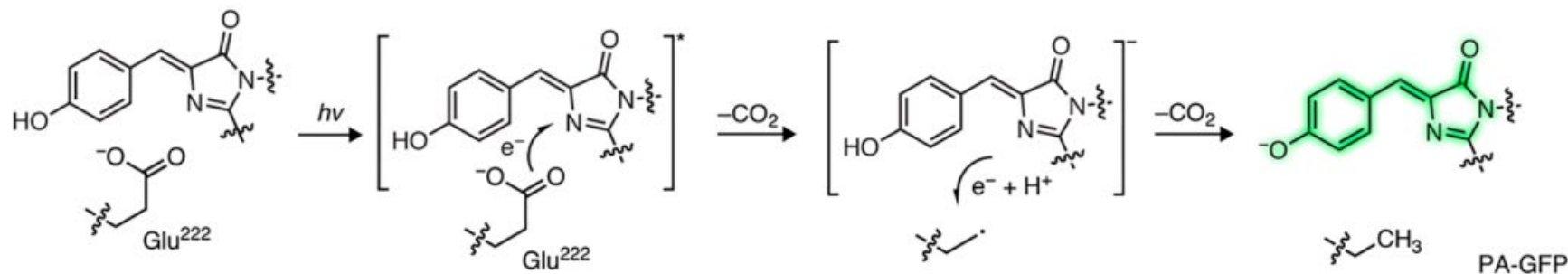
High absorption coefficient and quantum yield to produce bright events.

Exceptional resistance to bleaching since tens of thousands of images are collected at high laser power.

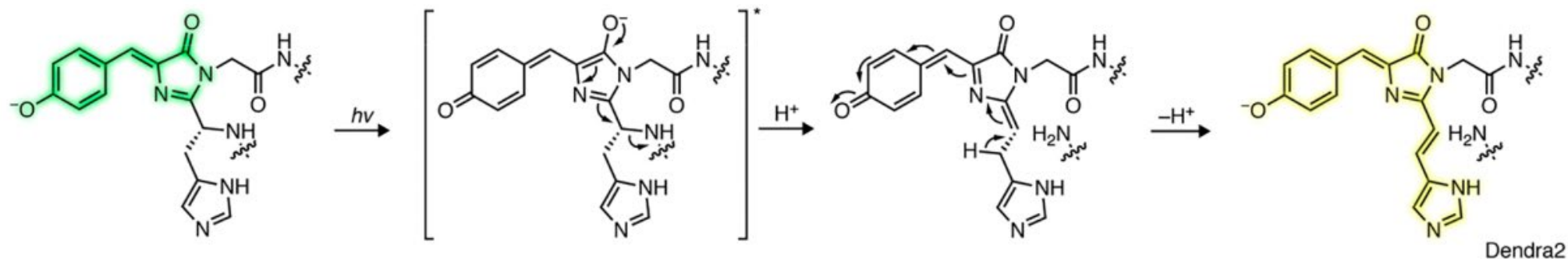
Bleaching, brightness, ON-time, and ON/OFF duty cycle are all strongly affected by laser power and buffer composition.

Photoswitchable Fluorescent Proteins

Photoactivation by decarboxylation (**PA-GFP**, PA-mKate, PA-mCherry)

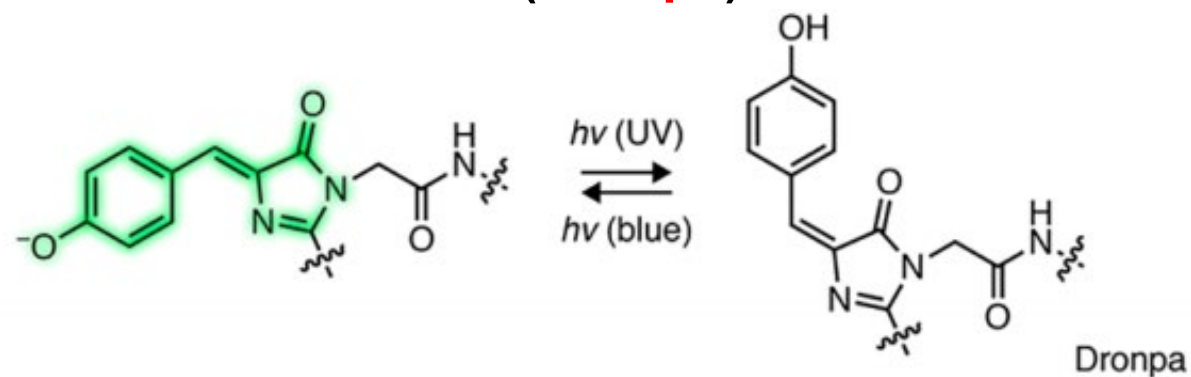


Photoswitching by beta-elimination (Dendra, **mEos**, mClavGR2, mlrisFP, mMaple)

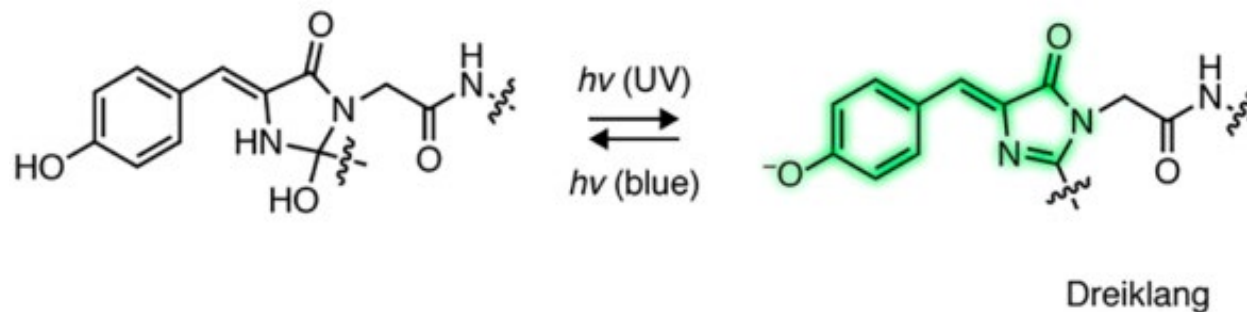


Photoswitchable Fluorescent Proteins












Photoconversion by *cis-trans* isomerization (**Dronpa**)



Photoconversion by hydration/dehydration (**Dreiklang**)



Photoswitchable Fluorescent Proteins

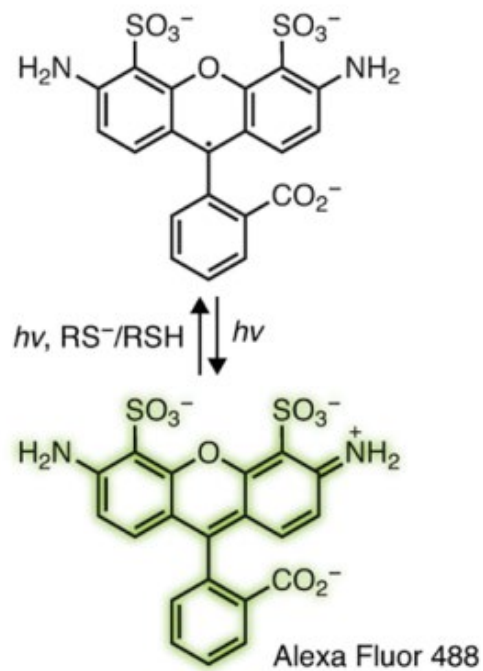
Name		$\epsilon \times 10^4$ (M ⁻¹ cm ⁻¹)	Φ	F_{on}/F_{off}	$t_{1/2}M^b$ (min)	$t_{1/2on}^c$ (s)	$t_{1/2PB}^c$ (s)	N	σ (nm)
<i>Photoactivatable</i>									
PA-GFP		1.74	0.79	60	<10	1.8	150	313 (\bar{x})	41 (\bar{x})
PAmCherry1		1.80	0.46	4000	23	2.5	100	724 (\bar{x}) 413 (M)	18 (\bar{x}) 17 (M)
PATagRFP		6.60	0.38	550	75	4.5	180	251–906 (\bar{x}) 150 (M)	39 (\bar{x}) 31 (M)
PAmKate		2.50	0.18	100	19	6.3	350	NR	15 (\bar{x})
<i>Photoswitchable</i>									
PS-CFP2		4.30; 4.70	0.20; 0.23	1000	NR	NR	NR	262–930 (\bar{x}) 250 (M)	29 (\bar{x}) 27 (M)
Dendra2		4.50; 3.50	0.50; 0.55	300	90	NR	260; 2420	131–686 (\bar{x})	23 (\bar{x})
mEos3.2		6.34; 3.22	0.84; 0.55	NR	20	NR	13; 48	482–809 (\bar{x}) 264 (M)	12 (\bar{x}) 10 (M)
mClavGR2		1.90; 3.20	0.77; 0.53	200	27	NR	233; 3644	379 (\bar{x})	<30(\bar{x})
mMaple3		1.50; 0.74	3.0; 0.56	400	49	NR	9.4;133	675 (\bar{x})	NR
PSmOrange		11.3; 3.3	0.51; 0.28	550	96	NR	15; 49	337 (\bar{x})	45 (\bar{x})

Name		$\epsilon \times 10^4$ (M ⁻¹ cm ⁻¹)	FR	ϕ	F_{on}/F_{off}	$t_{1/2}M^b$ (min)	$t_{1/2}on^c$ (s)	$t_{1/2}off^c$ (s)	$t_{1/2}PB^c$ (s)	N	σ (nm)	
<i>Photochromic</i>												
bsDronpa		4.5	100	0.50	20	NR	0.04	1.25	12.5	560 (\bar{x})	<45(\bar{x})	
rsEGFP		4.7	1200	0.36	65	120	0.00002	0.001	800	<60 (\bar{x})	70 (\bar{x})	
Skylan-S		15.2	7000	0.64	26	NR	0.073	4.77	NR	NR	20 (\bar{x})	
mGeos-M		5.2	8	0.85	20	<10	NR	21.03	20	458 (\bar{x}) 387 (M)	14 (\bar{x}) 12 (M)	
Dronpa		9.5	4	0.85	20	25	0.12	115	2	299 (\bar{x}) 269 (M)	17(\bar{x}) 15 (M)	
rsFastlime		4.6	35	0.60	65	NR	0.03	2.60	65	<60 (\bar{x})	40 (\bar{x})	
Padron		4.3	15	0.64	140	NR	5.6	0.06	40	NR	NR	
Drieklang		8.3	160	0.41	20	120	1	3	21	720 (\bar{x})	15 (\bar{x})	
rsTagRFP		3.7	75	0.11	20	43	0.0028	0.18	NR	NR	NR	
rsCherry		8.0	50	0.02	10	NR	3.0	0.05	NR	359 (\bar{x}) 288 (M)	24 (\bar{x}) 22 (M)	
rsCherryRev		8.4	400	0.005	10	42	0.05	0.7	NR	401 (\bar{x}) 264 (M)	25 (\bar{x}) 23 (M)	

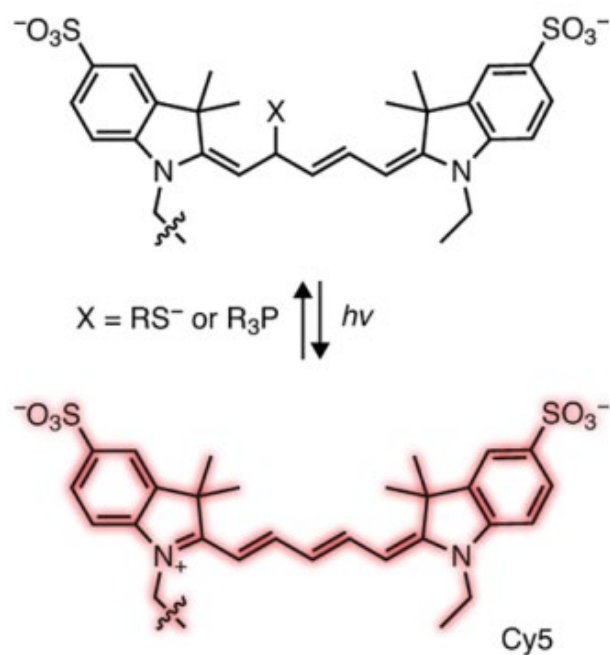
Photoswitchable Dyes

Conventional fluorophores (**Alexa Fluor 488**, **Cy5**, **Cy3**)

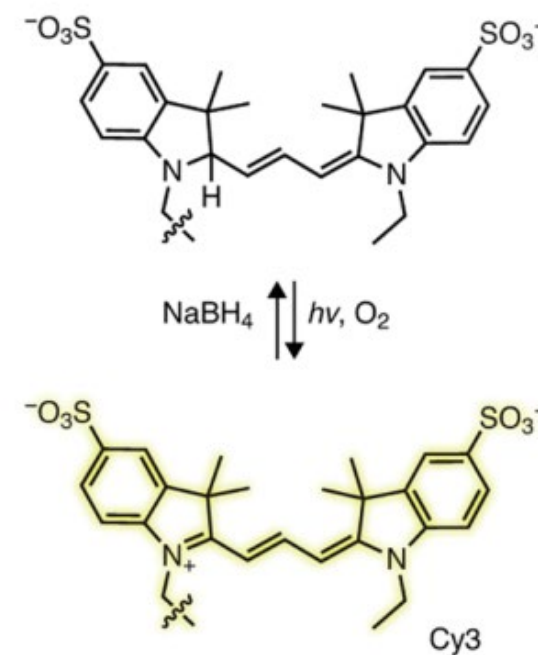
Redox-switching (*d*STORM)



Thiol or phosphine adducts



Reduction

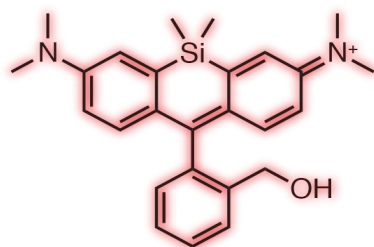
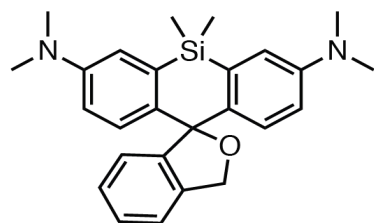


Photoswitchable Dyes

Spontaneously blinking (**HM-SiR**)

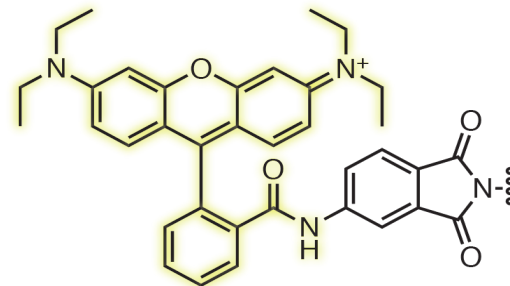
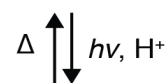
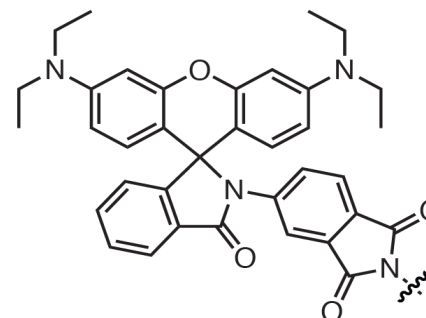
Photochromic rhodamines

Hydroxymethyl Rhodamines



HM-SiR

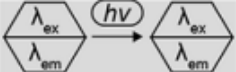







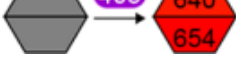




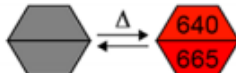
Rhodamine lactams



Rh_B phthalimide

Photoswitchable Dyes

Name		$\epsilon \times 10^4$ ($M^{-1}cm^{-1}$)	ϕ	$t_{1/2on}$ (s)	$t_{1/2off}$ (s)	N	σ (nm)	
<i>Activator-reporter pairs</i>								
Cy3-Cy5		25	0.28	1.0	1.0	3000 (\bar{x})	NR	
Name		$\epsilon \times 10^4$ ($M^{-1}cm^{-1}$)	ϕ	on/off $\times 10^{-5}$	SC	SF	N^b	σ (nm)
<i>Activator free</i>								
ATTO 488		9	0.80	220	49	0.99	1110 (\bar{x})	29
Cy3B		13	0.67	40	5	0.89	2057 (\bar{x})	22
Alexa Fluor 647		24	0.33	120	26	0.73	5202 (\bar{x})	17
DyLight750		22	NR	20	6	0.58	749 (\bar{x})	30

Name		$\epsilon \times 10^4$ ($M^{-1}cm^{-1}$)	Φ	on/off $\times 10^{-5}$	Φ_{PA}	N	σ (nm)
<i>Photoactivatable/Caged</i>							
Rhodol-NN		9	0.3	NR	0.16	NR	36
PA-JF ₅₄₉		9	0.78	10	0.022	637 (\bar{x})	14
PA-JF ₆₄₆		12	0.47	0.16	NR	760 (\bar{x})	21
N ₃ -DCDHF		5	0.03–0.4 ^c	NR	0.095	1100 (\bar{x})	18
NVOC ₂ -Rh _Q		9.9	0.83	NR		540 (\bar{x})	NR
NVOC ₂ -Rh ₁₁₀		7.6	0.88 ^d	NR		3488 (\bar{x})	16
NVOC ₂ -OG		8.2	0.97	NR	0.0013	235 (\bar{x})	NR
NVOC ₂ -SiRh _Q		8	0.38	NR		14944 (\bar{x})	5
<i>Photochromic</i>							
OA-2		8	0.09	NR	0.02	600 (\bar{x})	70
Rh _B phthalimide		10	0.31	NR	NR	900 (\bar{x})	55
Rh _B stilbene		10	0.31	NR	0.009	3800 (\bar{x})	13-17
DAE-sulfone		5.4	0.34	NR	0.0065	200–350 (\bar{x})	70
<i>Spontaneously blinking</i>							
HMSiR		10	0.39	NR	NR	2600 (\bar{x})	52

Current Approaches in SMLM

They differ primarily in how ON/OFF switching is achieved:

(f)PALM – photoactivation

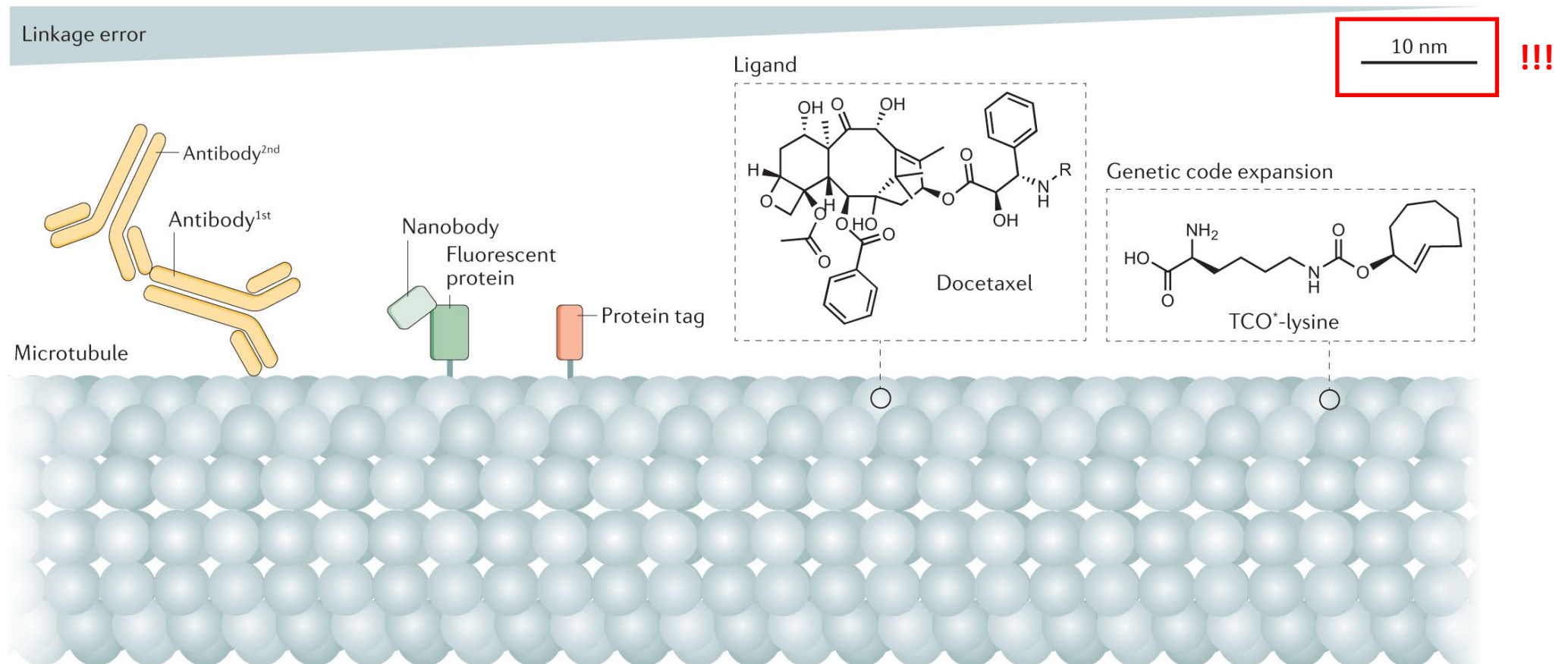
STORM – photoswitching of activator and reporter dye-pair

dSTORM – conventional fluorescent probes in the presence of thiols transfer dyes to a long-lived OFF state

(f)BALM – binding and fluorescence activation of specific dyes

DNA-PAINT/Exchange-PAINT – transient oligonucleotide hybridization

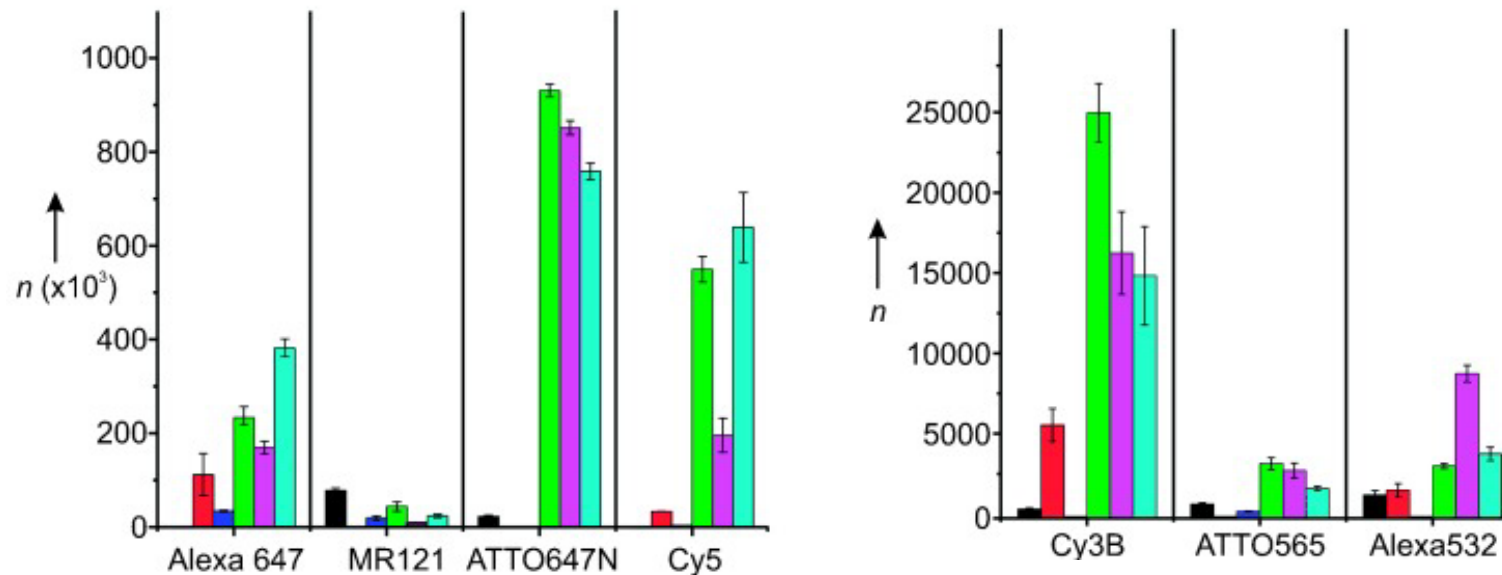
Linkage errors of various fluorescent labelling approaches



Buffers in SMLM

Different dyes blink optimally in different imaging buffers. Therefore, the acquisition of good quality 2- and 3-color images can be challenging.

Average photon counts per molecule in different buffers



Buffers in SMLM

Angewandte Chemie
DOI: 10.1002/anie.200801518

Fluorescence Spectroscopy

A Reducing and Oxidizing System Minimizes Photobleaching and Blinking of Fluorescent Dyes*

Jan Vogelsang, Robert Kasper, Christian Steinhilber, Britta Person, Mike Heilmann, Markus Sauer, and Philip Tinnefeld*

The exquisite selectivity, sensitivity obtained with fluorescence spectroscopy led to an ever-increasing number of applications and sophisticated detection schemes and sophisticated detection schemes in current fluorescence microscopy which pose severe limitations on blinking. Most of the basic dye still used in fluorescence microscopy are used in the development of the latest high-resolution applications¹⁻³ in the form of new kinds of emitters such as crystal, silver nanodusters, and cent proteins^{4,5}. In comparison, the organic dyes such as rhodamine have been incremental device since

Controlling the fluorescence of ordinary oxazine dyes for single-molecule switching and superresolution microscopy

Jan Vogelsang, Thorben Cordes, Carsten Forthmann, Christian Steinhilber, and Philip Tinnefeld*

Angewandte Physik-Biophysik und Center for NanoScience, Ludwig-Maximilians-Universität, Amalienstrasse 54, 80799 Munich, Germany

Fluorescent molecular switches have widespread potential for use as sensors, material applications in electro-optical data storage and

Commonly unwanted and uncontrolled switching between bright ("on") and dark ("off") states is observed in single-molecule (SM) experiments. Dark states often originate from triplet state (T₁) or from radical transfer reactions (R-21) along the underlying (rod-like) axis photobleaching as well as (T₁) spin control over blinking of the first reduced state and so, which stabilizes the reduced (of molecular oxygen that we experiments. We presumed that thermally stable, switching is DNA-oxazine constructs (ox-21708) in aqueous solution from reducing for switching on. We used single-molecule fluorescence correlation spectroscopy (FCS) to study the photophysical pathways of these DNA-oxazine constructs. Besides an intriguing switching mechanism (switching kinetics) that is based on the subsequent recombination of the reduced state, the importance of dark fluorescence microscopy using has been realized (2, 24, 25). The

ANNUAL REVIEW

Click here for quick links to Annual Reviews content online, including:

- Top cited articles
- Top downloaded articles
- Our comprehensive search

Photophysics of Fluorescent Probes for Single-Molecule Biophysics and Super-Resolution Imaging

Tackjip Ha^{1,2} and Philip Tinnefeld¹

CONTENTS

ANNUAL REVIEW

BRIEF COMMUNICATIONS

Cyanine fluorophore derivatives with enhanced photostability

Roger B Altman¹, Daniel S Terry^{2,7}, Zhou Zhou^{1,2,7}, Qinsi Zheng³, Peter Geggier⁴, Rachel A Kolster⁴, Yongfang Zhao⁵, Jonathan A Javitch^{4,5}, David Warren⁶ & Scott C Blanchard^{1,3,6}

Fluorescence applications requiring high photostability often depend on the use of solution additives to enhance fluorophore performance. Here we demonstrate that the direct or proximal conjugation of cyclooctatetraene (COT), 4-nitrobenzyl alcohol (NBA) or Trolox to the cyanine fluorophore Cy5 dramatically enhanced fluorophore photostability without otherwise affecting its native spectral characteristics. Such conjugation is a powerful means of improving the robustness of fluorescence-based applications demanding long-lived, nonblinking fluorescence emission.

Small organic fluorophores are powerful research tools in biological imaging that have enabled unprecedented insights into both cellular and molecular processes. However, their performance can be compromised by undesirable photophysical properties that limit both the fluorescence quantum yield and the total number of photons emitted before photobleaching. Such issues include both transient (blinking) and irreversible (photobleaching) light

Despite their advantages, TSQs have key limitations, including poor aqueous solubility, problems with membrane permeability and biological toxicity. To circumvent these issues, here we show that direct or proximal linkage of TSQs to the Cy5 fluorophore reduced blinking and photobleaching in both deoxygenated and oxygenated environments to extents exceeding those using TSQs in solution. We also observed enhanced Cy5 performance in living cells, suggesting these new fluorophore derivatives may be valuable for *in vivo* applications⁷.

In vitro single-molecule studies demonstrating that TSQs operate in a concentration-dependent fashion to affect the photophysical properties of cyanine fluorophores⁸ suggest a collision-based mode of action⁹. To determine whether additional enhancements in fluorophore performance could be achieved by increasing the effective TSQ concentration beyond the solubility limit while simultaneously bypassing issues related to toxicity, we synthesized specific Cy5-TSQ conjugates in which we directly linked COT, NBA or Trolox to the fluorophore through a flexible, 12-atom linker (Supplementary Fig. 1). We developed a general strategy for the synthesis of such compounds by first modifying each TSQ to contain a single, amine-functional group followed by coupling it to the commercially available, bis-reactive, N-hydroxysuccinimide ester (NHS)-Cy5 fluorophore to yield a mono-functionalized NHS-Cy5-TSQ species at high efficiency (~30–60%) and purity (>98%) (Fig. 1a and Supplementary Note).

Bulk fluorescence measurements of the TSQ-conjugated Cy5 fluorophores demonstrated that absorption and emission spectra of TSQ-fluorophore conjugates were largely indistinguishable from those of the parent Cy5 compound, aside from modest shifts in fluorescence quantum yield (Supplementary Fig. 2a,b). The quan-

Journal of Biotechnology 140 (2010) 260–266

Contents lists available at ScienceDirect

Journal of Biotechnology

journal homepage: www.elsevier.com/locate/jbiotec

The effect of photoswitching kinetics and labeling densities on super-resolution fluorescence imaging

Sebastian van de Linde^a, Steve Wolter^a, Mike Heilmann^{b,c}, Markus Sauer^{a,*}

^a Biotechnology and Biophysics, Julius-Maximilians-University Würzburg, Am Hubland, 97074 Würzburg, Germany

^b Applied Laser Physics and Laser Spectroscopy and Bertold Institute for Biophysics and Neuroscience, Bertold Institute, Universitätstrasse 25, 21033 Bielefeld, Germany

ARTICLE INFO

Received 4 November 2009
Received in revised form 19 February 2010
Accepted 15 February 2010

ABSTRACT

Keywords: Molecular photoswitches; Super-resolution imaging; STORM; Diffraction limit; Single-molecule based localization microscopy

DOI: 10.1002/jbtec.201000189

Make them Blink: Probes for Super-Resolution Microscopy

Jan Vogelsang,^{1,2} Christian Steinhilber,^{2,3} Carsten Forthmann,^{2,3} Ingo H. Stein,^{2,3} Britta Person-Skegro,^{2,3} Thorben Cordes,² and Philip Tinnefeld^{1,2}

In recent years, a number of approaches have emerged that enable far-field fluorescence imaging beyond the diffraction limit of light, namely super-resolution microscopy. These techniques are beginning to profoundly alter our abilities to look at biological structures and dynamics and are bound to spread into conventional biological laboratories. However, these ap-

proaches have been used for localization-based super-resolution microscopy techniques and outline the special requirements for the fluorescent probes used in combination with the advances in understanding the photophysics and photochemistry of single fluorophores, we demonstrate how essentially any single-molecule compatible fluorophore can be used for super-

provides an overview of recent developments in super-resolution microscopy techniques and outline the special requirements for the fluorescent probes used in combination with the advances in understanding the photophysics and photochemistry of single fluorophores, we demonstrate how essentially any single-molecule compatible fluorophore can be used for super-

ANALYSIS

Evaluation of fluorophores for optimal performance in localization-based super-resolution imaging

Graham T Dempsey^{1,6}, Joshua C Vaughan^{2,3,6}, Kok Hao Chen^{3,6}, Mark Bates⁴ & Xiaowei Zhuang^{2,3,5}

One approach to super-resolution fluorescence imaging uses sequential activation and localization of individual fluorophores to achieve high spatial resolution. Essential to this technique is the choice of fluorescent probes: the properties of the probes, including photons per switching event, on-off duty cycle, photostability and number of switching cycles, largely dictate the quality of super-resolution images. Although many probes have been reported, a systematic characterization of the properties of these probes and their impact on super-resolution image quality has been described in only a few cases. Here we quantitatively characterized the switching properties of 26 organic dyes and directly related these properties to the quality of super-resolution images. This analysis provides guidelines for characterization of super-resolution probes and a resource for selecting probes based on performance. Our evaluation identified several photostable dyes with good to excellent performance in four independent spectral ranges, with which we demonstrated low-cross-talk, four-color super-resolution imaging.

STORM concept is also applicable to other photoswitchable fluorophores and fluorescent proteins.¹⁰ Indeed, a variety of fluorescent probes have been used for localization-based super-resolution imaging, including organic dyes^{1,6–9}, fluorescent proteins^{4,11,22,23} and quantum dots²⁴. In the simplest imaging mode, continuous illumination of a single dye (for example, Alexa Fluor 647) with a single laser wavelength can generate high-quality STORM images, where the laser accomplishes all three tasks of activating the dye to the fluorescent state, exciting fluorescence from the dye and switching it off to the dark state¹⁴. As Alexa Fluor 647, a variety of commonly used organic dyes spanning a broad spectrum of colors can transition between fluorescent and dark states and have been used for super-resolution imaging^{10,11,14–16}. Depending on the fluorophore probe used, this imaging method has also been referred to by several other names (for example, direct (d)STORM^{11,15}), which use the same fundamental imaging principle as STORM, a technique generally applicable to photoswitchable probes.

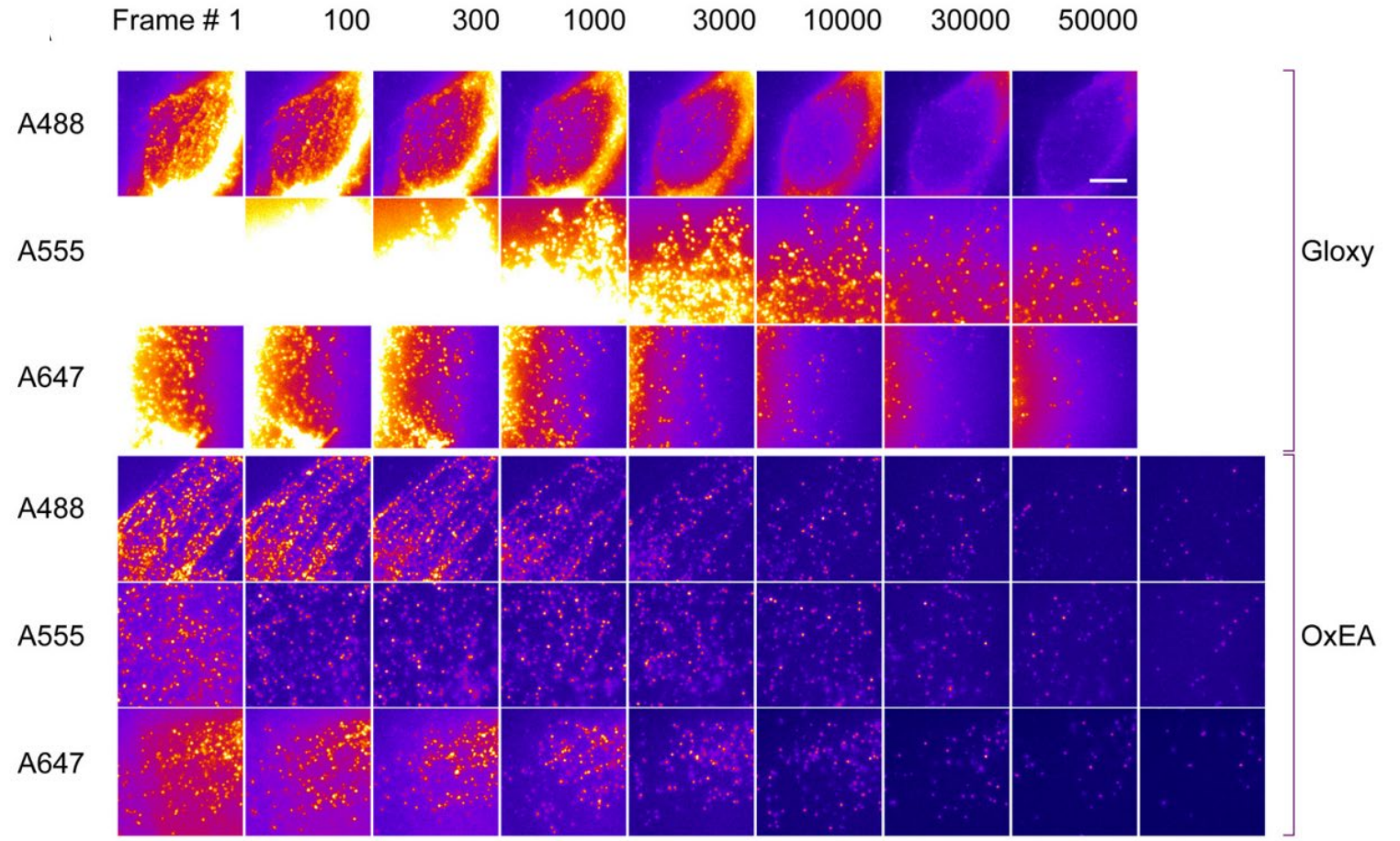
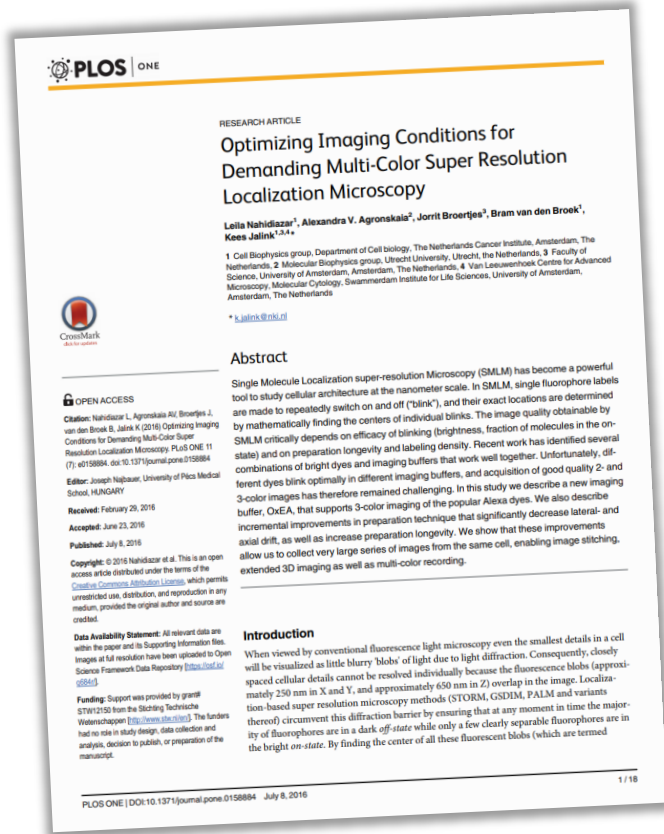
The photoswitchable probes can be largely divided into two categories (Fig. 1b): (i) reversibly switchable probes that can be converted between fluorescent (on) and dark (off) states multiple times upon excitation by light either of the same or different wavelengths and (ii) irreversibly activatable probes that exist initially in a dark state and can be activated by light to a fluorescent state. Examples in the first category include photoswitchable cyanine, rhodamine and oxazine dyes^{3,6,7,16,15,18} and photoswitch-

The spatial resolution limit of light microscopy imposed by diffraction has recently been overcome by super-resolution fluorescence imaging methods^{1–3}. Among these methods, stochastic optical reconstruction microscopy (STORM)³ and (fluorescence) photoactivated localization microscopy^{1,5} can be used to achieve sub-diffraction-limit resolution by sequen-

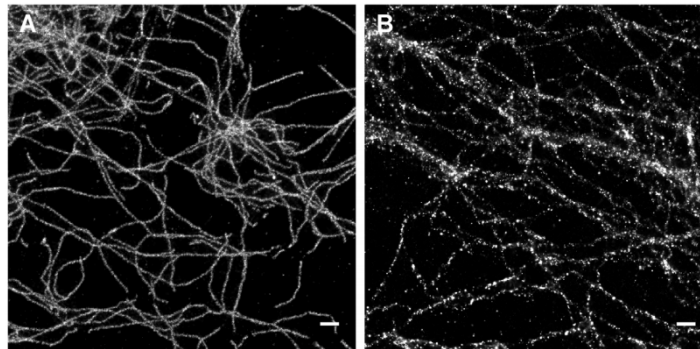
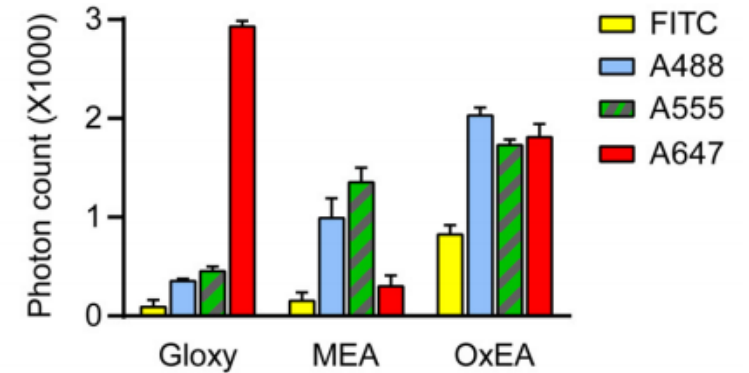
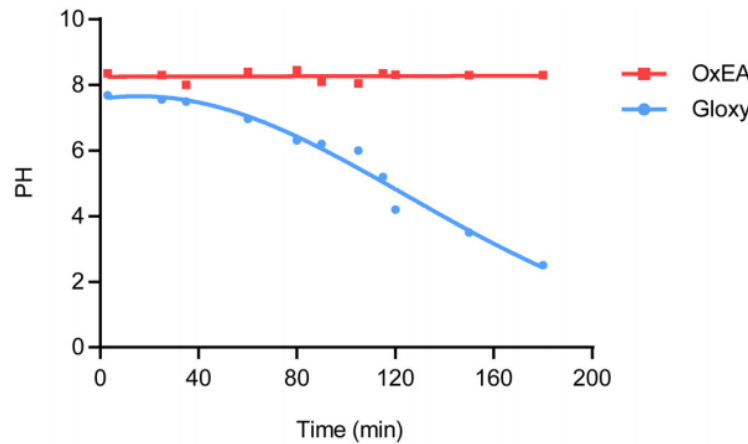
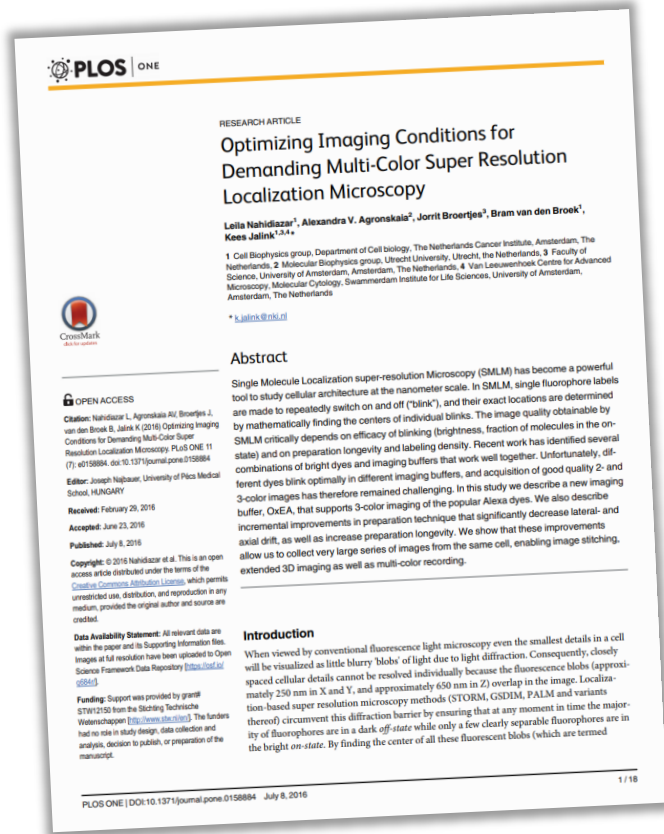
© 2010 Nature America, Inc. All rights reserved.

Advice: Once you have picked a dye for your SMLM experiment depending on your microscope (available lasers) and biological constraints, make yourself familiar with which buffers are most suitable and test & optimize them.

Buffers in SMLM






Buffers in SMLM



Comparison of image quality in ageing Gloxy buffer (B) to that in OxEA buffer (A).

Advice: Always prepare your imaging buffer right before experiments & adjust your imaging buffer choice for multicolor experiments.

Overview

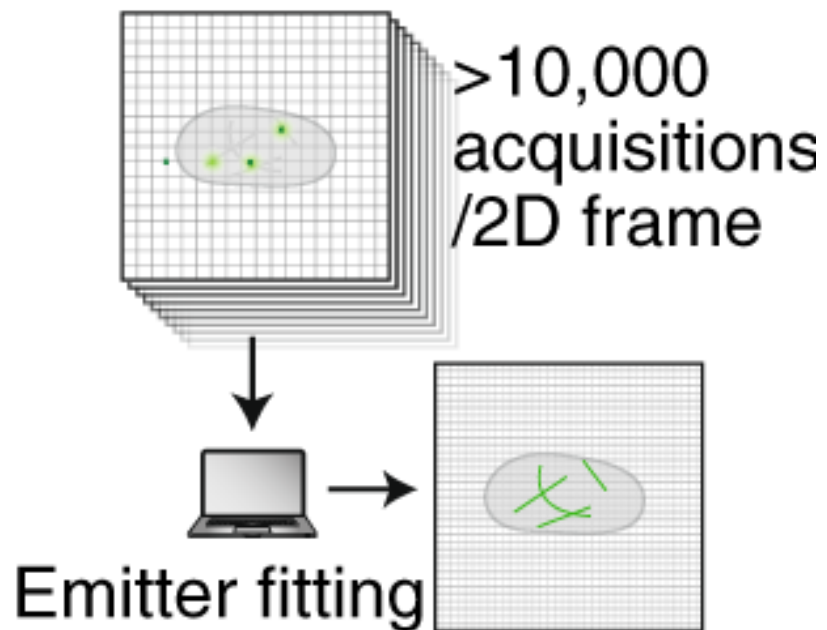
- Basic principles 2D SMLM 
- Hardware for SMLM 
- Practical considerations: sample preparation, suitable dyes, linkage errors, and buffers 
- Processing, quantification, and interpretation of SMLM data
- 3D SMLM
- Summary

- Extra: New directions in SMLM
- Extra: SRM as a multidimensional challenge

Processing, quantification, and interpretation of SMLM data

How large is an SMLM dataset?

50,000 frames taken with a 16-bit camera (1024 x 1024 pixel) lead to...



Total number of pixel on the detector:

$$1024 \times 1024 = 1,048,576 \text{ pixel}$$

Total bits:

$$1,048,576 \times 16 \text{ bits} = 16,777,216 \text{ bits}$$

Conversion into bytes:

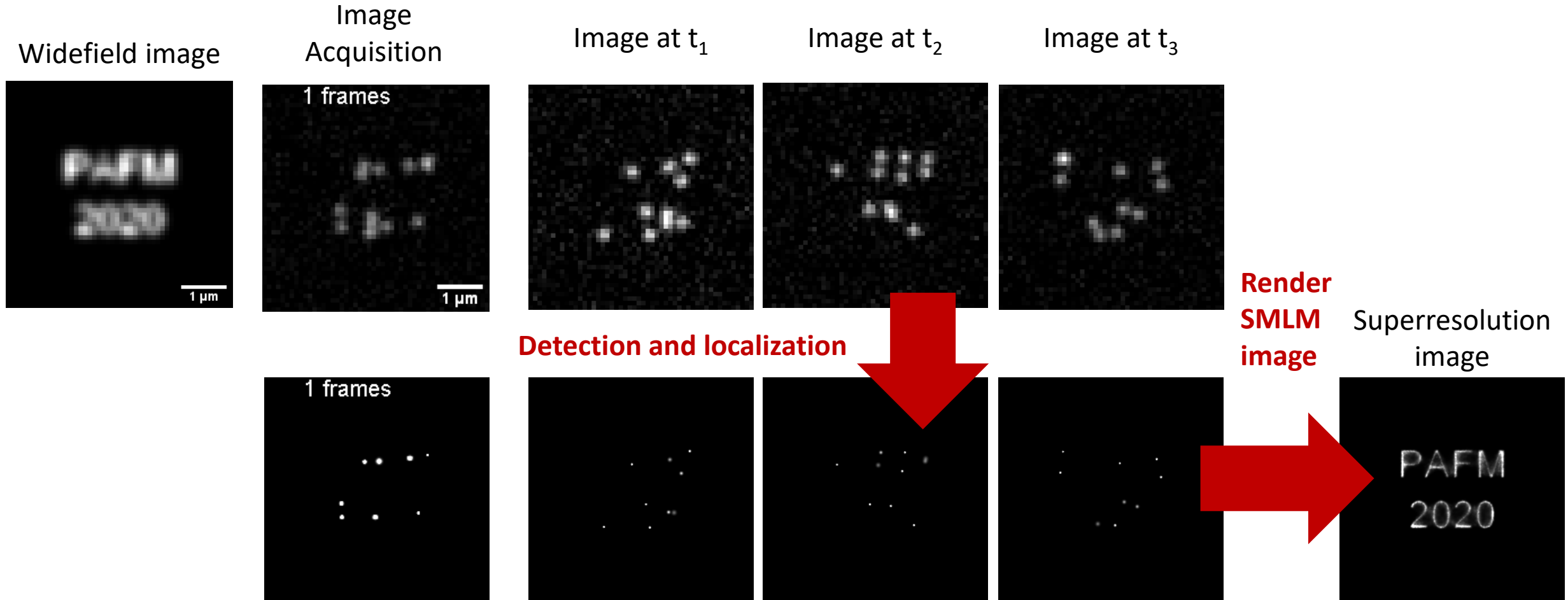
$$16,777,216 \text{ bits} / 8 = 2,097,152 \text{ bytes} \\ \sim 2 \text{ MB (one frame)}$$

Upscaled to 50,000 frames:

$$2 \text{ MB} \times 50,000 \sim \mathbf{100 \text{ GB}}$$

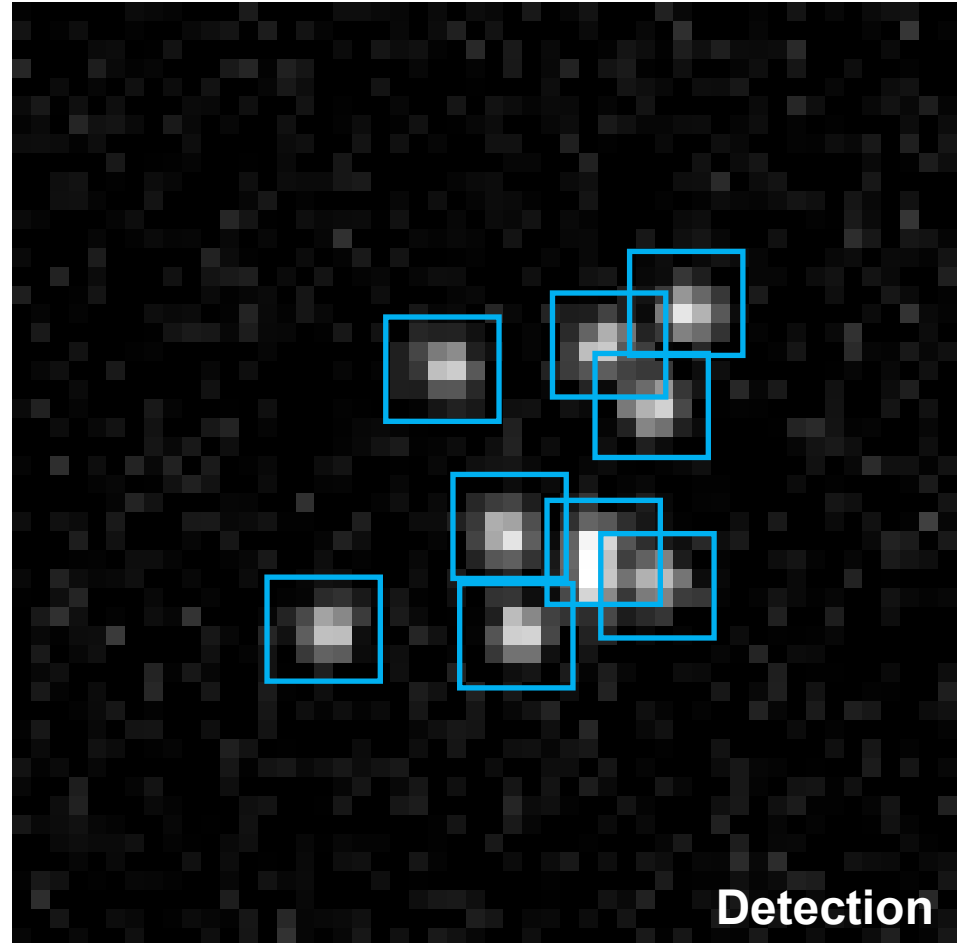
That is a lot of data that needs to be handled...

From raw SMLM data to reconstructed super-resolved image



Detection

- Approximate molecule location
= Detection

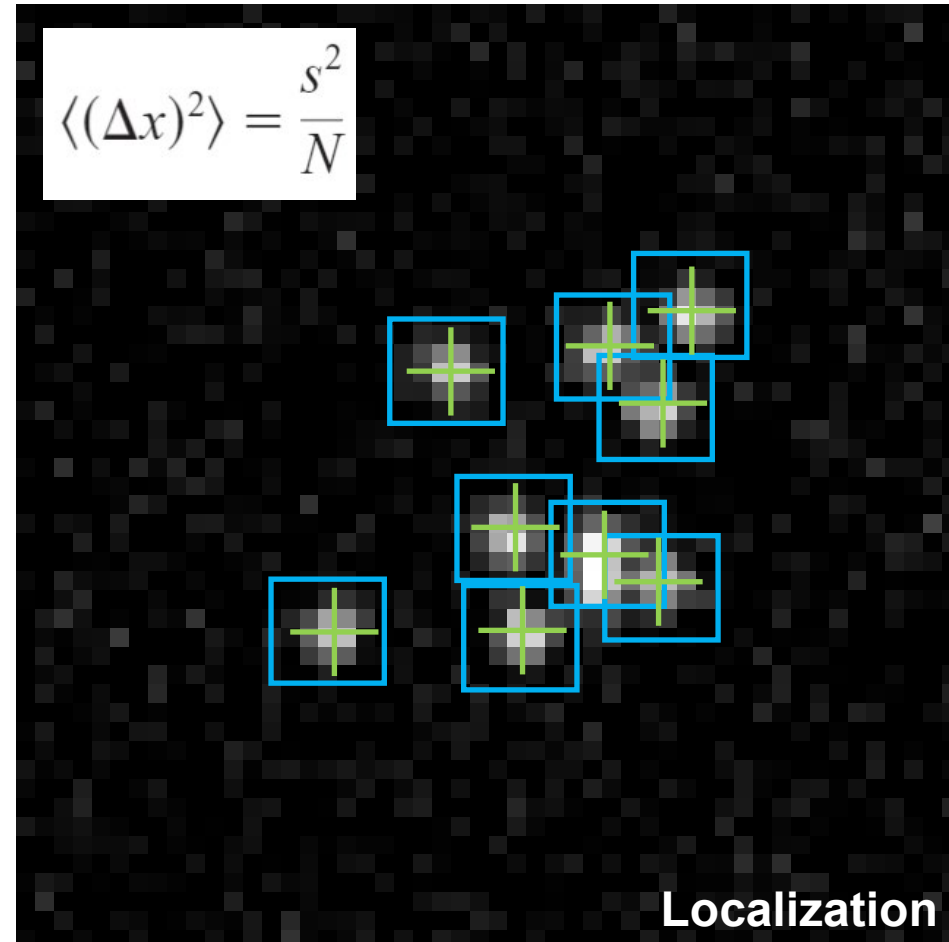


Detection and localization

$$\Delta x \approx \frac{\lambda}{2NA} \quad \text{Abbe Equation}$$

vs.

- Approximate molecule location
= Detection
- Accurate determination of the
molecule center
= Localization



Biophysical Journal Volume 82 May 2002 2775-2783

2775

Precise Nanometer Localization Analysis for Individual Fluorescent Probes

Russell E. Thompson, Daniel R. Larson, and Watt W. Webb
Cornell University, School of Applied and Engineering Physics, Ithaca, New York 14853 USA

ABSTRACT Calculation of the centroid of the images of individual fluorescent particles and molecules allows localization and tracking in light microscopes to a precision that is limited by factors that limit the precision of these techniques (e.g., photon shot noise, pixel size, and detector noise). In this paper, we describe a method for localization that is robust over a wide range of conditions. In a series of simulations, we constructed and tested both on image stacks of simulated particles and actual images. The availability of a simple equation for the quality of an experimental apparatus and in di-

$$\langle(\Delta x)^2\rangle = \frac{s^2 + a^2/12}{N} + \frac{4\sqrt{\pi} s^3 b^2}{aN^2}$$

Error in localization – Equations

$$\langle (\Delta x)^2 \rangle = \frac{s^2}{N}$$

Δx Error in localization

s Standard deviation of the PSF

N Number of photons collected

The modified equation to account for photon-counting noise, pixelation noise and background noise:

$$\langle (\Delta x)^2 \rangle = \frac{s^2 + a^2/12}{N} + \frac{4\sqrt{\pi} s^3 b^2}{aN^2}$$

a Size of the pixel

b Background noise

Detection and localization

- Approximate molecule location
= Detection
- Accurate determination of the
molecule center
= Localization



- Result: List of localizations (x,y
coordinates, localization errors /
uncertainties & add. parameters)

New images with localizations?



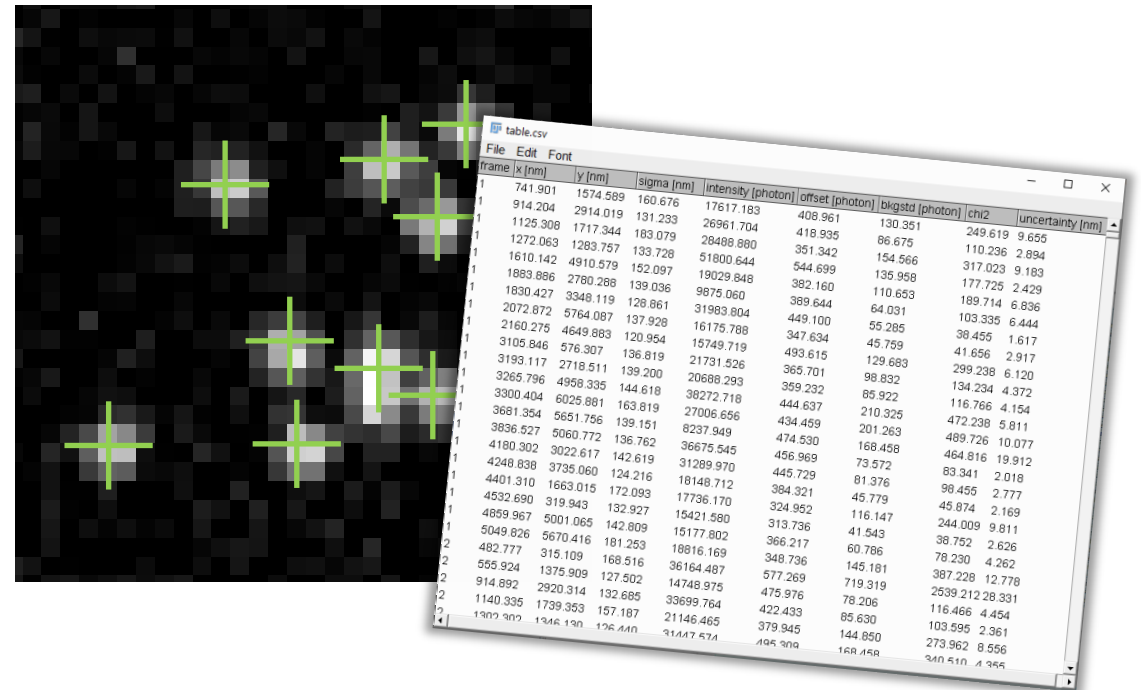
No, but a list of localizations!

Pixel data vs. point clouds

In contrast to standard microscopy imaging that produces 2D pixel or 3D voxel grid data, SMLM generates big data of 2D or 3D point clouds with millions of localizations and associated uncertainties.

Therefore, processing, quantification, analysis and interpretation of SMLM must be approached differently.

To this day, the SMLM data quantification and interpretation methods have yet to keep pace with the rapid advancement of SMLM imaging.



List of localizations

frame	x [nm]	y [nm]	sigma [nm]	intensity [photon]	offset [photon]	bkgstd [photon]	chi2	uncertainty [nm]
1	741.901	1574.589	160.676	17617.183	408.961	130.351	249.619	9.655
1	914.204	2914.019	131.233	26961.704	418.935	86.675	110.236	2.894
1	1125.308	1717.344	183.079	28488.880	351.342	154.566	317.023	9.183
1	1272.063	1283.757	133.728	51800.644	544.699	135.958	177.725	2.429
1	1610.142	4910.579	152.097	19029.848	382.160	110.653	189.714	6.836
1	1883.886	2780.288	139.036	9875.060	389.644	64.031	103.335	6.444
1	1830.427	3348.119	128.861	31983.804	449.100	55.285	38.455	1.617
1	2072.872	5764.087	137.928	16175.788	347.634	45.759	41.656	2.917
1	2160.275	4649.883	120.954	15749.719	493.615	129.683	299.238	6.120
1	3105.846	576.307	136.819	21731.526	365.701	98.832	134.234	4.372
1	3193.117	2718.511	139.200	20688.293	359.232	85.922	116.766	4.154
1	3265.796	4958.335	144.618	38272.718	444.637	210.325	472.238	5.811
1	3300.404	6025.881	163.819	27006.656	434.459	201.263	489.726	10.077
1	3681.354	5651.756	139.151	8237.949	474.530	168.458	464.816	19.912
1	3836.527	5060.772	136.762	36675.545	456.969	73.572	83.341	2.018
1	4180.302	3022.617	142.619	31289.970	445.729	81.376	98.455	2.777
1	4248.838	3735.060	124.216	18148.712	384.321	45.779	45.874	2.169
1	4401.310	1663.015	172.093	17736.170	324.952	116.147	244.009	9.811
1	4532.690	319.943	132.927	15421.580	313.736	41.543	38.752	2.626
1	4859.967	5001.065	142.809	15177.802	366.217	60.786	78.230	4.262
1	5049.826	5670.416	181.253	18816.169	348.736	145.181	387.228	12.778
2	482.777	315.109	168.516	36164.487	577.269	719.319	2539.212	28.331
2	555.924	1375.909	127.502	14748.975	475.976	78.206	116.466	4.454
2	914.892	2920.314	132.685	33699.764	422.433	85.630	103.595	2.361
2	1140.335	1739.353	157.187	21146.465	379.945	144.850	273.962	8.556
2	1302.302	1346.130	126.440	31447.574	495.309	168.458	340.510	4.955

x,y – central coordinate

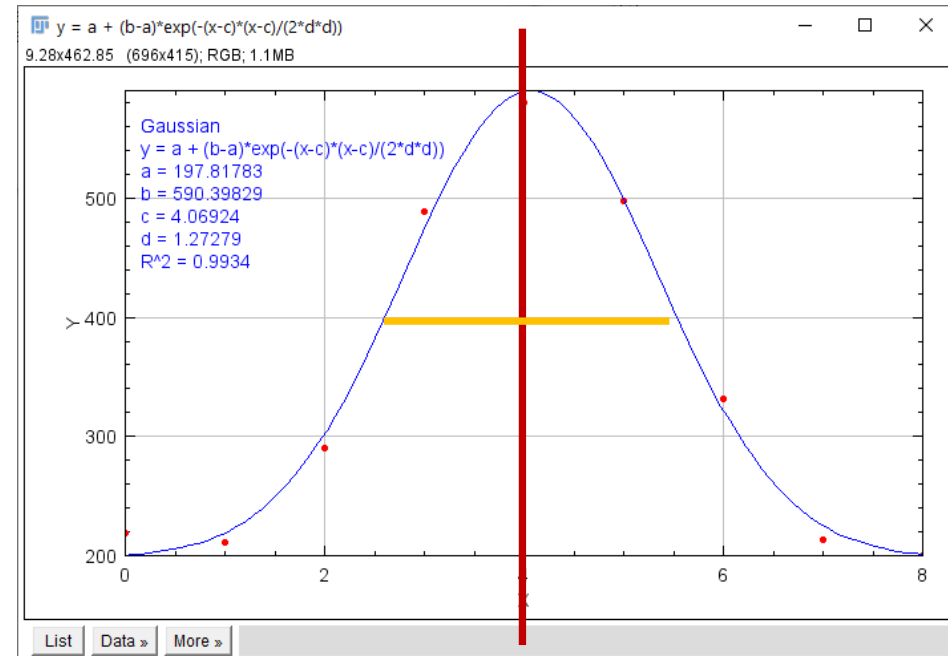
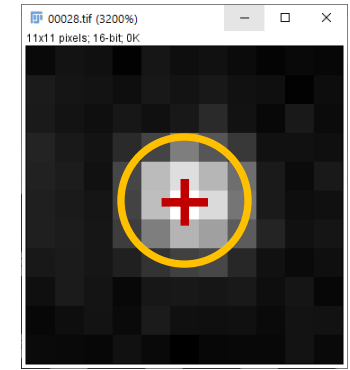
sigma - Gaussian width

Gaussian amplitude / offset

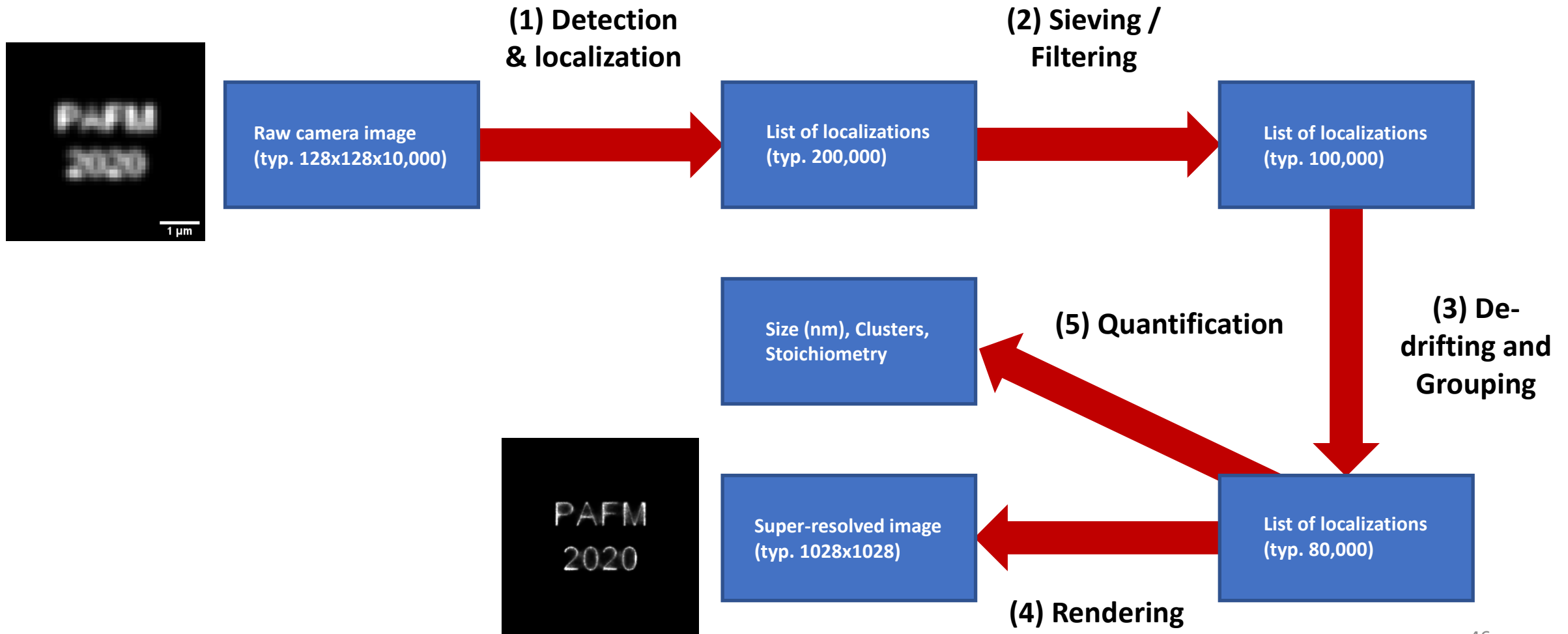
χ² – goodness-of-fit

Uncertainty

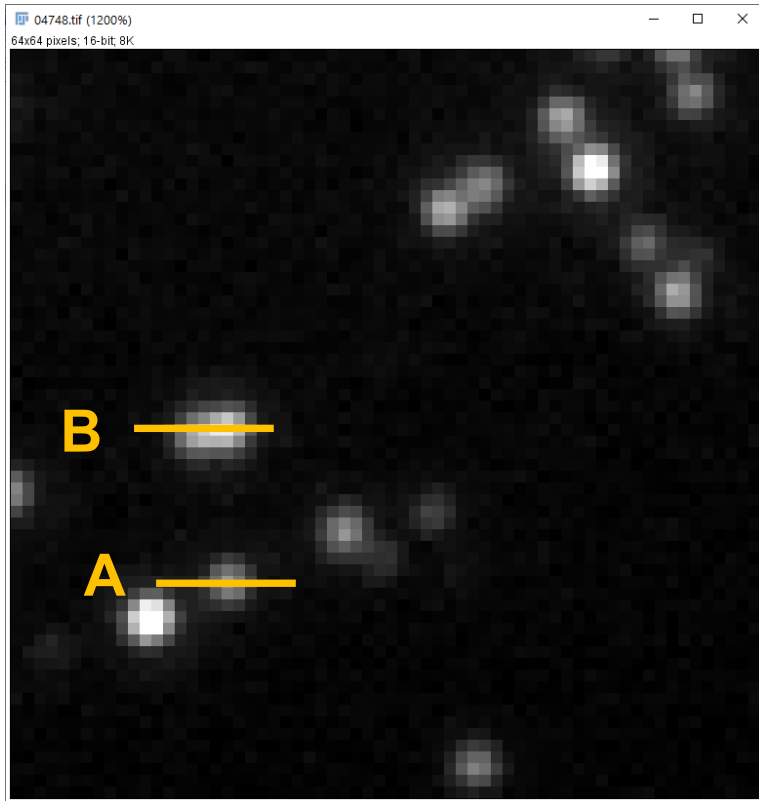
$$\langle(\Delta x)^2\rangle = \frac{s^2 + a^2/12}{N} + \frac{4\sqrt{\pi} s^3 b^2}{aN^2}$$



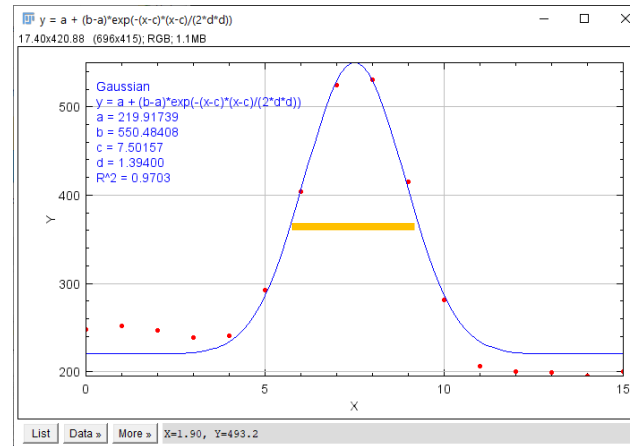
Sequence of SMLM processing and analysis steps



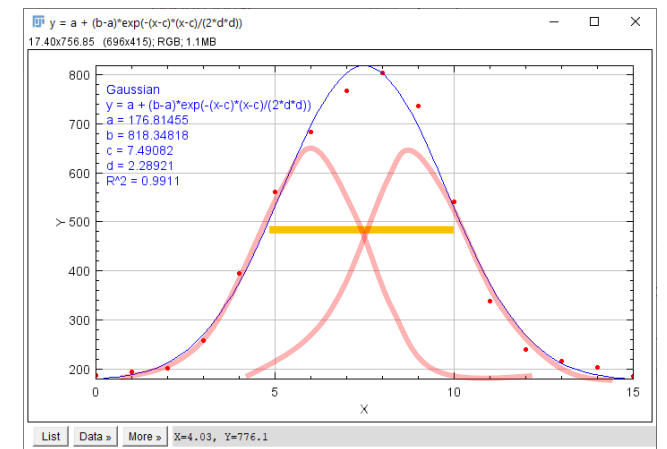
High-density data / multiple emitters



A

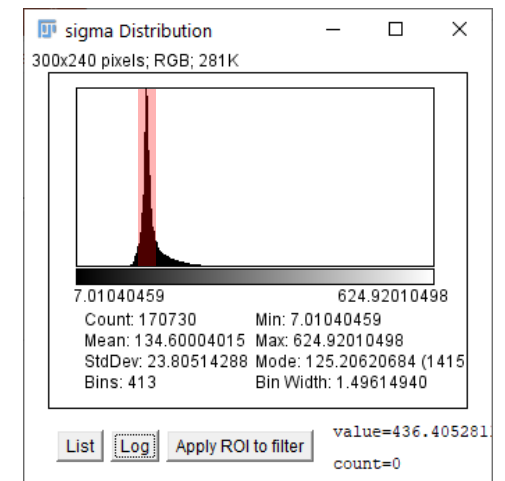


B



Choosing a suitable multi-emitter fitting method/algorithm can help to deal with high-density data.

Alternatively, you can filter/sieve your data to handle invalid localizations.

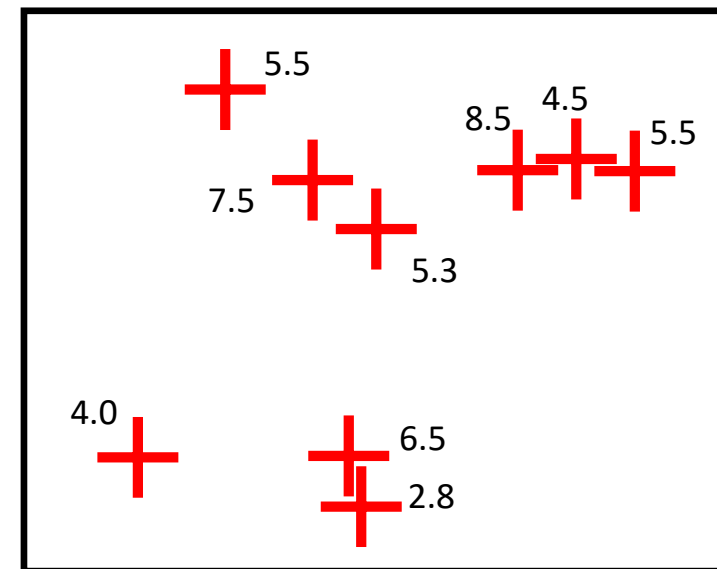
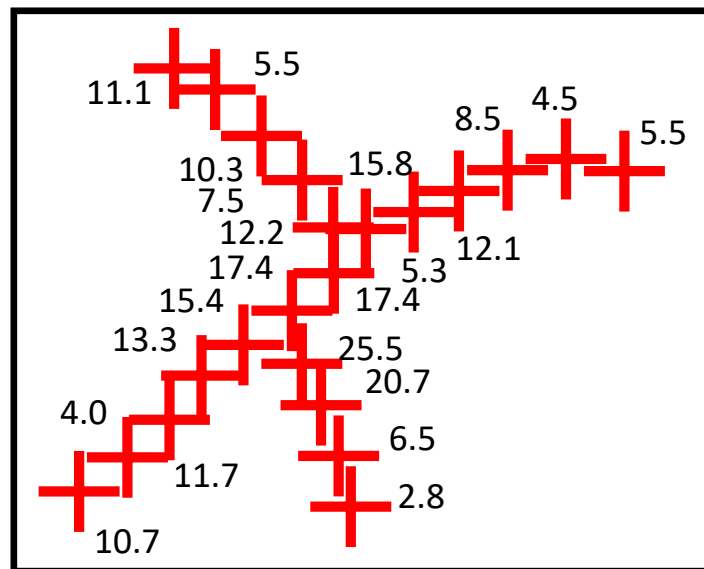
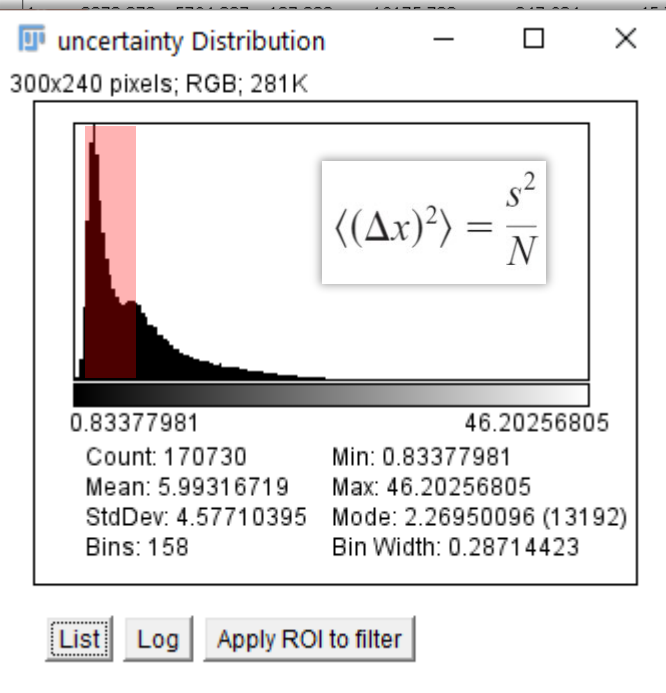


Advice: Choose suitable filtering parameters with the histogram of the respective fitting parameter.

SMLM's resolution

frame	x [nm]	y [nm]	sigma [nm]	intensity [photon]	offset [photon]	bkgstd [photon]	chi2	uncertainty [nm]
1	741.901	1574.589	160.676	17617.183	408.961	130.351	249.619	9.655
1	914.204	2914.019	131.233	26961.704	418.935	86.675	110.236	2.894
1	1125.308	1717.344	183.079	28488.880	351.342	154.566	317.023	9.183
1	1272.063	1283.757	133.728	51800.644	544.699	135.958	177.725	2.429
1	1610.142	4910.579	152.097	19029.848	382.160	110.653	189.714	6.836
1	1883.886	2780.288	139.036	9875.060	389.644	64.031	103.335	6.444
1	1830.427	3348.119	128.861	31983.804	449.100	55.285	38.455	1.617

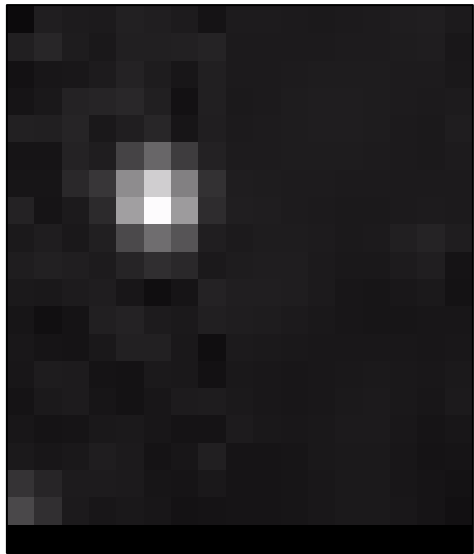
So, when you filter/sieve out high uncertainties, you can reach insanely high resolutions, right? **No, not really!**



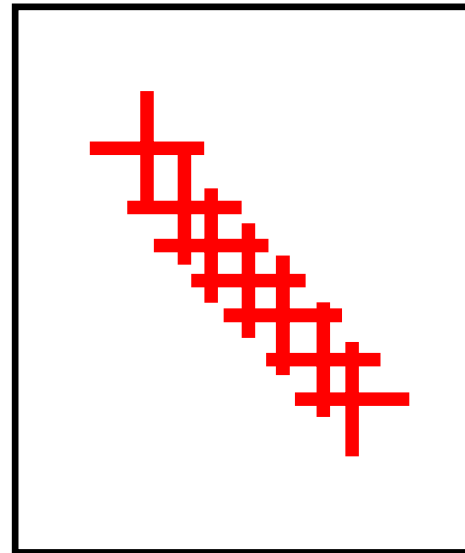
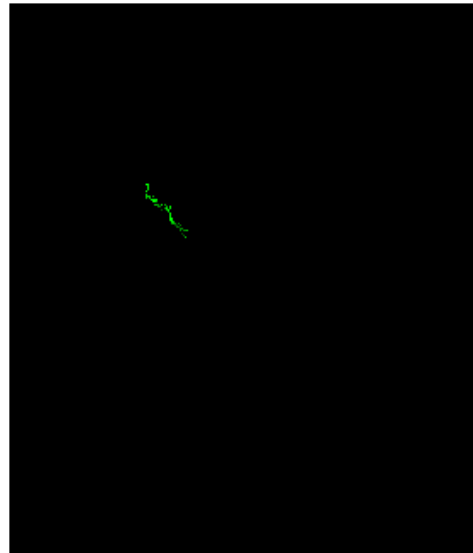
You can filter high uncertainties, but at a certain point you'll lose the structure's integrity. The measure of resolution would be meaningless.

Drift-correction

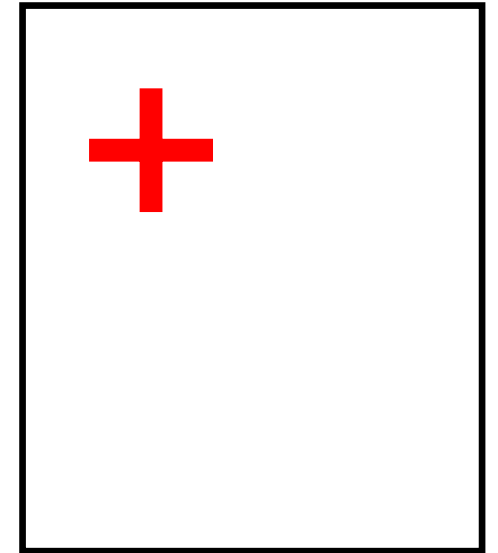
4 min movie



0.5 μm



uncorrected

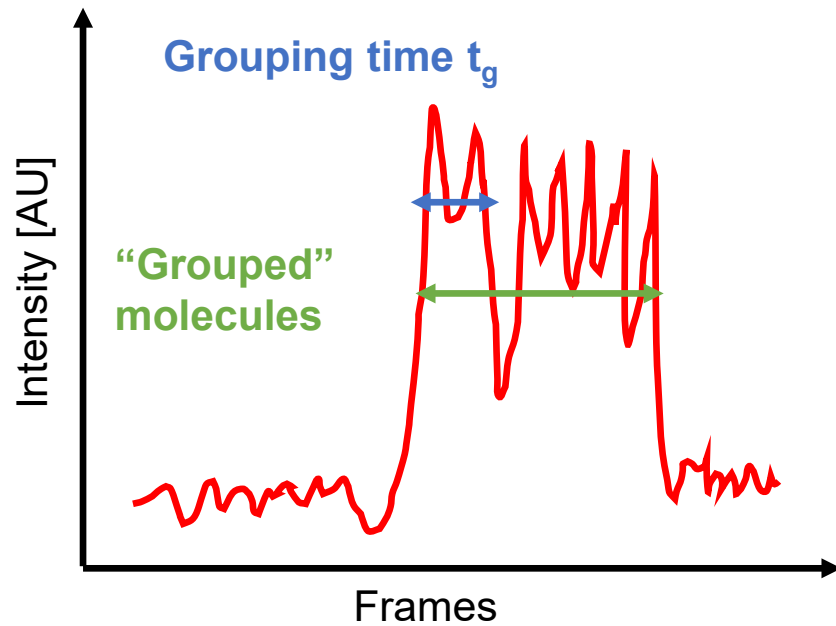


corrected

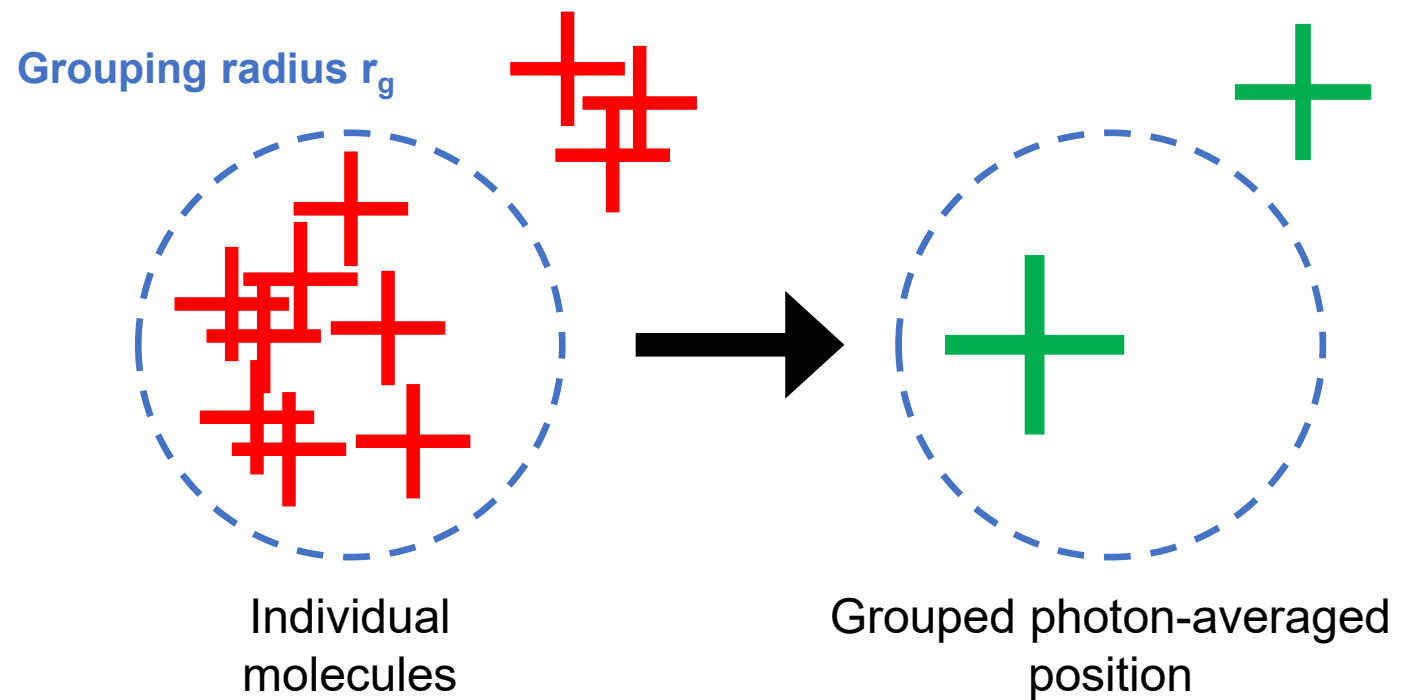
Drift becomes a limiting factor in achieving high resolution. Fortunately, it can be corrected for by fiducial-based or image-based (cross-correlation) strategies.

Grouping / Blink-correction

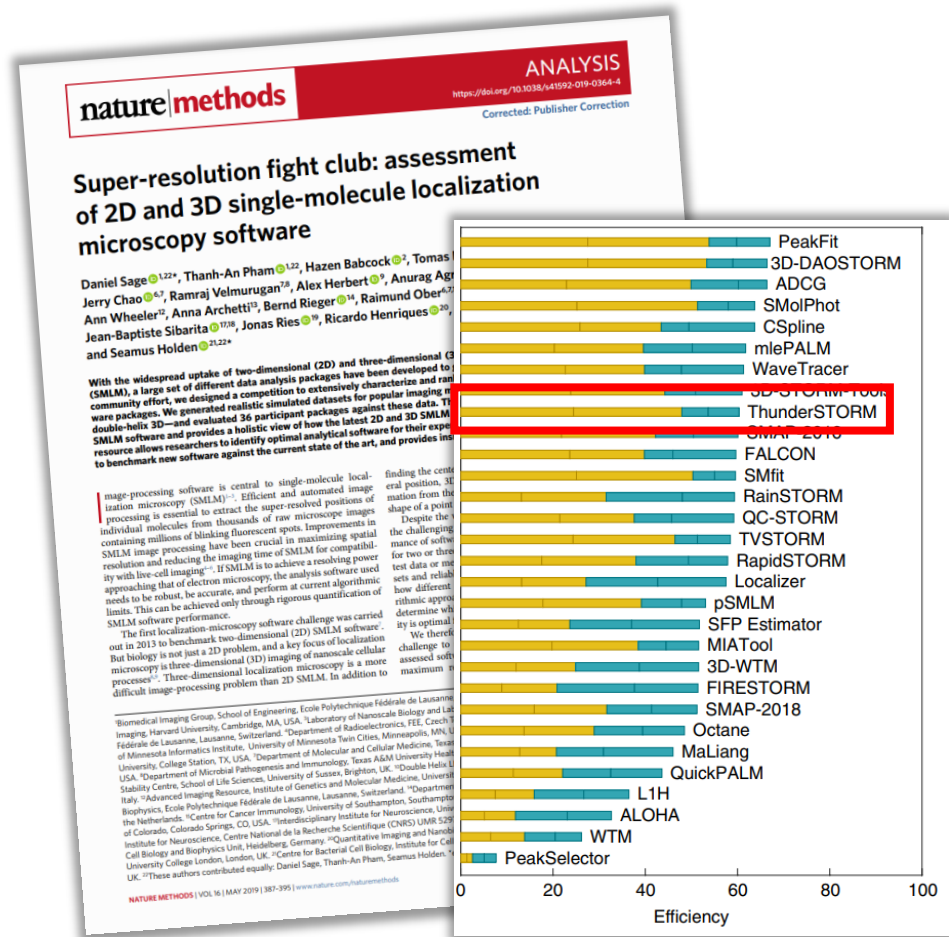
According to time



According to space

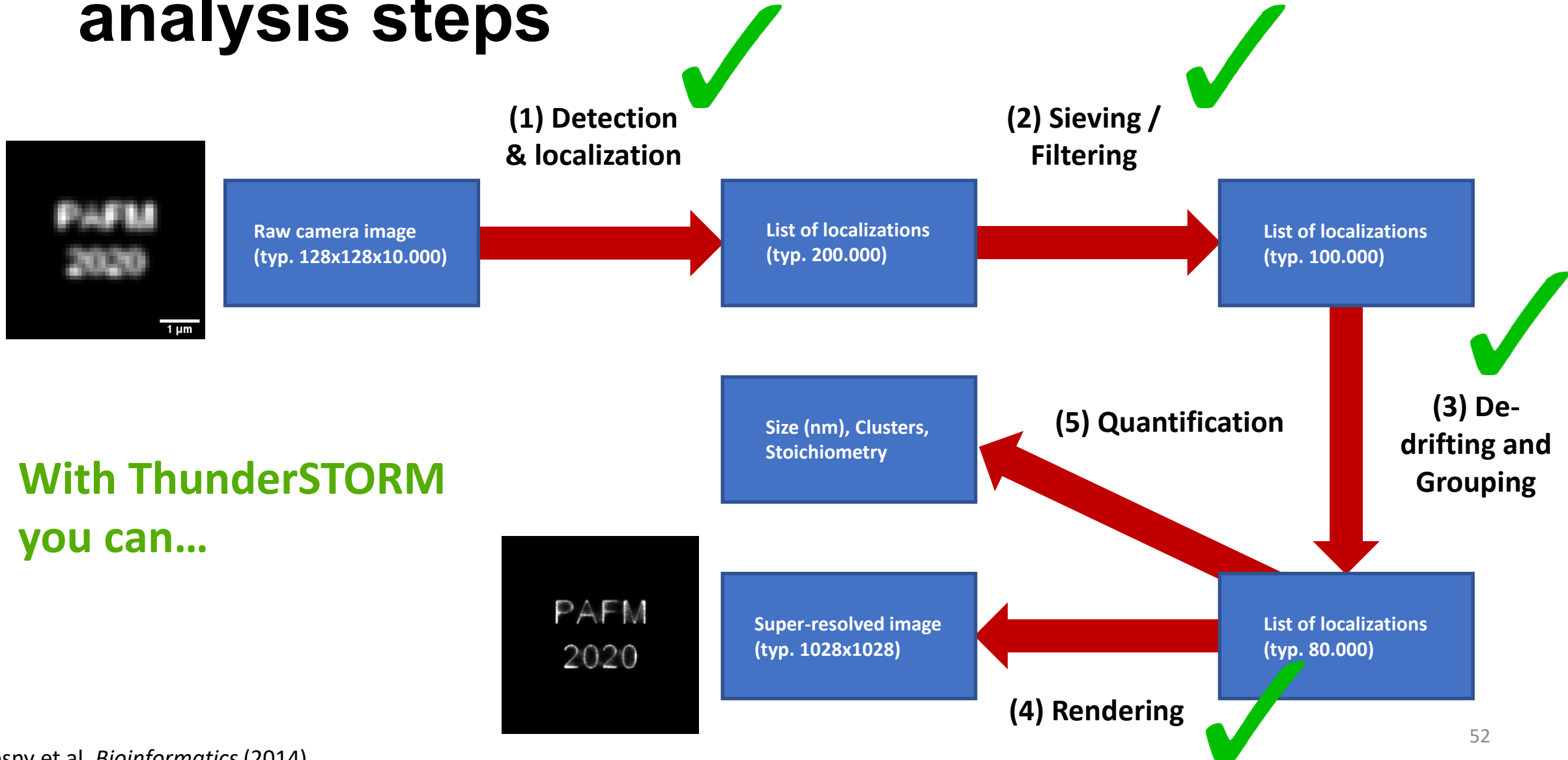


Software for SMLM



Software	Molecule detection	PSF	Method	Platform	Acc.
3D-DAOSTORM ²⁸	Adaptive threshold—update on residual images	Gauss	LS	Python	+
a-livePALM ²⁹	Denoising, SNR threshold, adaptive histogram equalization	Gauss	MLE	Matlab	+
Auto-Bayes	Generalized minimum-error threshold (GMET), local maximum	Gauss, Weibull	LS	Stand-alone	+
B-recs	Detection: n/a; fit: Bayesian inference framework	Arbitrary	MMSE, MAP	Stand-alone	-
CSSTORM ³⁰	No explicit localization; convex optimization problem (HD)	Gauss	Compressed sensing	Matlab	+
DAOSTORM ³¹	Gaussian filtering, local maximum (HD)	Measured, arbitrary	LS	Python	+
FacePALM ³²	No explicit localization; background estimation	—	—	Python	-
FALCON ³³	Deconvolution with sparsity prior, local maximum (HD)	Taylor approx.	ADMM	Matlab	+
Fast-ML-HD ³⁴	Sparsity constraint, concave-convex procedure (HD)	Gauss	MLE	Matlab	-
FPGA ³⁵	Adaptive threshold	Gauss	MLE, CoMass	Stand-alone	-
Gauss2DCirc ³⁶	Fixed SNR threshold	Gauss	REG	Matlab	+
GPUgaussMLE ³⁷	Simple (unspecified) methods to select subregions	Gauss	MLE	Matlab	+
GraspJ ³⁸	Peak finding: fixed threshold value	Gauss	MLE	ImageJ	+
Insight3	Low-pass filtering, local maximum	Arbitrary	LS	Stand-alone	-
L1H ³⁹	No explicit localization; L1 homotopy, FIST deconvolution	Gauss, arbitrary	Compressed sensing	Python	+
M2LE ⁴⁰	Adaptive threshold	Gauss	MLE	ImageJ	+
Maliang ⁴¹	Annular averaging filters, denoising by convolution	Gauss	MLE	ImageJ	+
Micro-Manager LM	Adaptive threshold	Gauss	LS	ImageJ	+
MrSE ⁴²	Band-pass filtering, local maximum	Radial	CoSym	Stand-alone	-
Octane ⁴³	Watershed maximum	Gauss	LS	ImageJ	+
PeakFit	Band-pass filtering, local maximum	Gauss	LS	ImageJ	+
PeakSelector ⁴⁴	Time-domain filtering, adaptive threshold	Gauss	LS	IDL, Matlab	-
PYME ²⁷	Wiener filtering, adaptive threshold	Arbitrary	LS	Python	+
QuickPALM ⁴⁵	Band-pass filtering, fixed SNR threshold	Gauss	CoMass	ImageJ	+
RadialSymmetry ⁴⁶	Filtering, local max., minimal distance to gradient	Radial	CoSym	Matlab	+
rapidSTORM ¹²	Low-pass filtering, local maximum	Gauss	LS, MLE	Stand-alone	+
SimplePALM ⁴⁷	Variance stabilization denoising, DoG, probabilistic threshold	n/a	Mean-shift	Stand-alone	-
simpleSTORM ¹⁴	Self-calibration, noise normalize, background subtraction, P value	Gauss, measured	Interpolation	Stand-alone	+
SNSMIL	Gaussian filtering, fixed contrast threshold	Gauss	LS	Stand-alone	+
SOSplugin	Wavelet transform, local maximum, Gaussian mixture	Gauss	LS	ImageJ	+
ThunderSTORM ¹⁵	Extensive collection of methods, preview, filtering, local maximum	Gauss	LS, MLE	ImageJ	+
W-fluoroBancroft ⁴⁸	Wavelet, adaptive threshold	Gauss	fB	Matlab	+
WaveTracer ⁴⁹	Wavelet, watershed maximum	Gauss	LS	Metamorph	-
WTM ⁵⁰	Wedge template matching (HD)	Wedge	Match.	Stand-alone	-

Sequence of SMLM processing and analysis steps



With ThunderSTORM
you can...



Feel free to test it...

Use the Fiji plugin ThunderSTORM to analysis the Tubulin 2D Long Sequence Dataset

Software: Fiji plugin ThunderSTORM

Plugin can be downloaded here:

<https://github.com/zitmen/thunderstorm/releases/tag/v1.3>

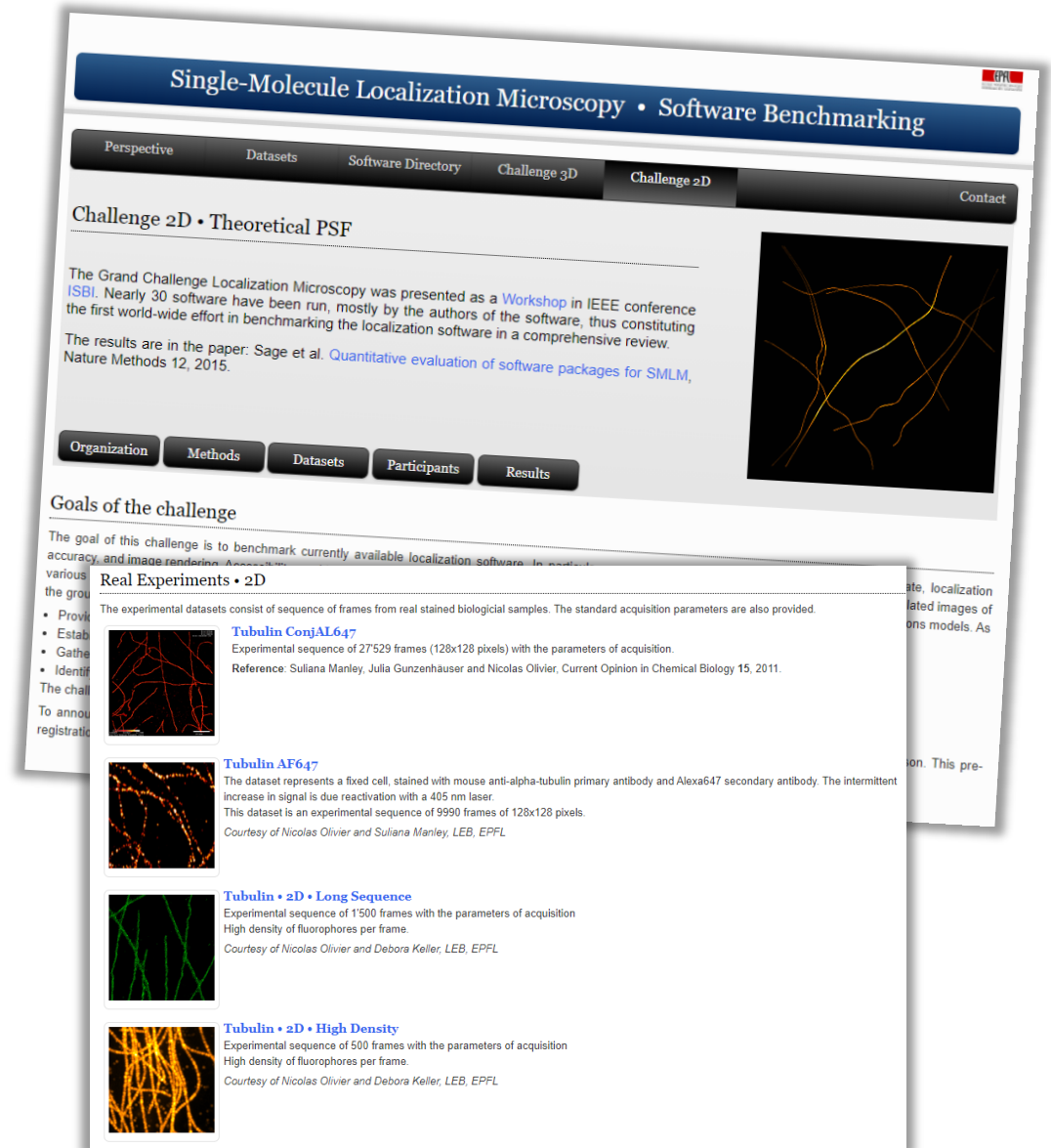
and will be located here: Plugins > ThunderSTORM

Online manual:

<https://github.com/zitmen/thunderstorm/wiki/Tutorials>

Dataset: Tubulin 2D Long Sequence

http://bigwww.epfl.ch/smlm/datasets/index.html?p=../challenge2013/datasets/Real_Long_Sequence



Single-Molecule Localization Microscopy • Software Benchmarking

Perspective Datasets Software Directory Challenge 3D Challenge 2D Contact

Challenge 2D • Theoretical PSF

The Grand Challenge Localization Microscopy was presented as a [Workshop](#) in IEEE conference [ISBI](#). Nearly 30 software have been run, mostly by the authors of the software, thus constituting the first world-wide effort in benchmarking the localization software in a comprehensive review.

The results are in the paper: Sage et al. [Quantitative evaluation of software packages for SMLM](#), Nature Methods 12, 2015.

Organization Methods Datasets Participants Results

Goals of the challenge

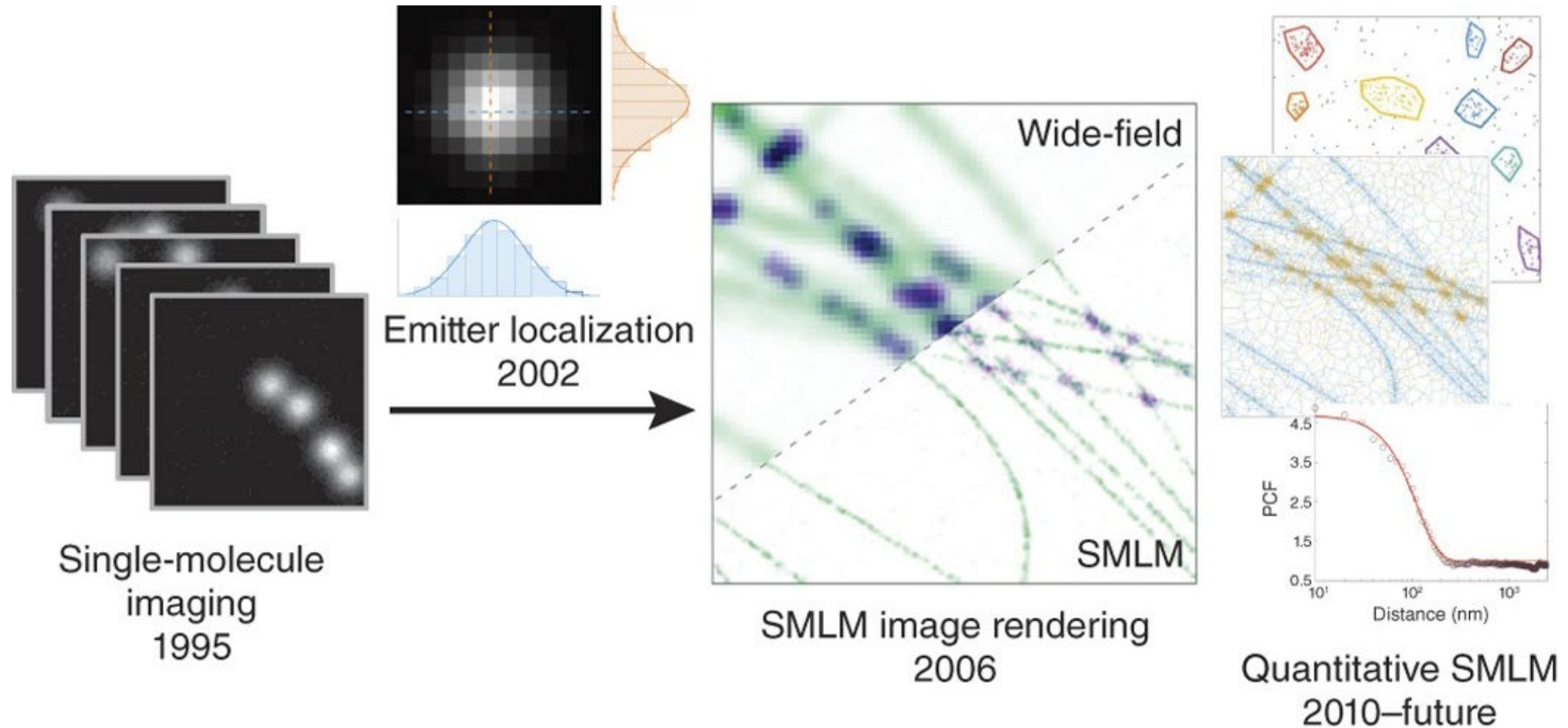
The goal of this challenge is to benchmark currently available localization software. In particular, accuracy and image rendering are the main focus.

Real Experiments • 2D

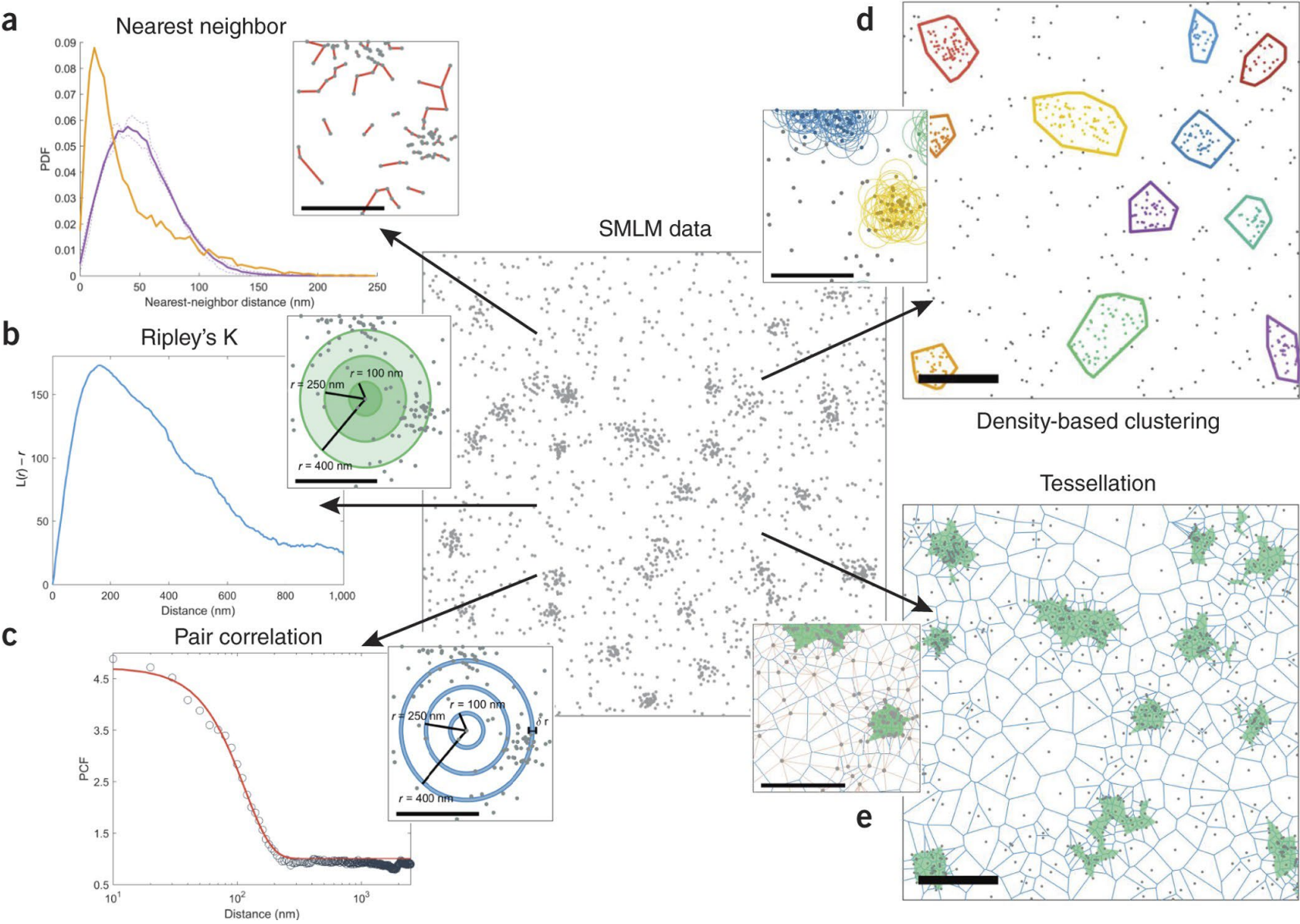
The experimental datasets consist of sequence of frames from real stained biological samples. The standard acquisition parameters are also provided.

- Tubulin ConjAL647**
Experimental sequence of 27529 frames (128x128 pixels) with the parameters of acquisition.
Reference: Suliana Manley, Julia Gunzenhäuser and Nicolas Olivier, Current Opinion in Chemical Biology 15, 2011.
- Tubulin AF647**
The dataset represents a fixed cell, stained with mouse anti-alpha-tubulin primary antibody and Alexa647 secondary antibody. The intermittent increase in signal is due reactivation with a 405 nm laser.
This dataset is an experimental sequence of 9990 frames of 128x128 pixels.
Courtesy of Nicolas Olivier and Suliana Manley, LEB, EPFL
- Tubulin • 2D • Long Sequence**
Experimental sequence of 1'500 frames with the parameters of acquisition
High density of fluorophores per frame.
Courtesy of Nicolas Olivier and Debora Keller, LEB, EPFL
- Tubulin • 2D • High Density**
Experimental sequence of 500 frames with the parameters of acquisition
High density of fluorophores per frame.
Courtesy of Nicolas Olivier and Debora Keller, LEB, EPFL

Timeline of SMLM developments







Spatial analysis approaches



Fiji plugins for SMLM post-processing

Name	Description	Year
bUnwarpJ	2D image registration; channel alignment by elastic transformation, deformations are represented by cubic B-splines	2006
ClearVolume	Multi-channel visualization package; rendering of image stacks for 3D and multi-colour representation	2015
FIRE	Resolution estimation; first ImageJ plugin for FRC analysis	2013
GDSC SMLM	Collection of plugins; many features such as drift correction, local density analysis, pair correlation analysis, and FRC	
MosaicIA	Cluster analysis; calculates an interaction potential that is most likely to generate the observed object distribution	2013
NanoJ-core	Drift correction and multi-colour channel alignment	2015
NanoJ-SQUIRREL	Benchmarking SMLM images; generates error map and FRC map, uncovers local differences in resolution	2018
QuASIMoDOH	Cluster analysis; divides images into tiles (tessellation), pattern analysis done by analysing the distribution of tile areas	2016
TRABI	Intensity analysis; macro that determines spot intensities in SMLM data by temporal analysis; can extract 3D information from 2D data	2017

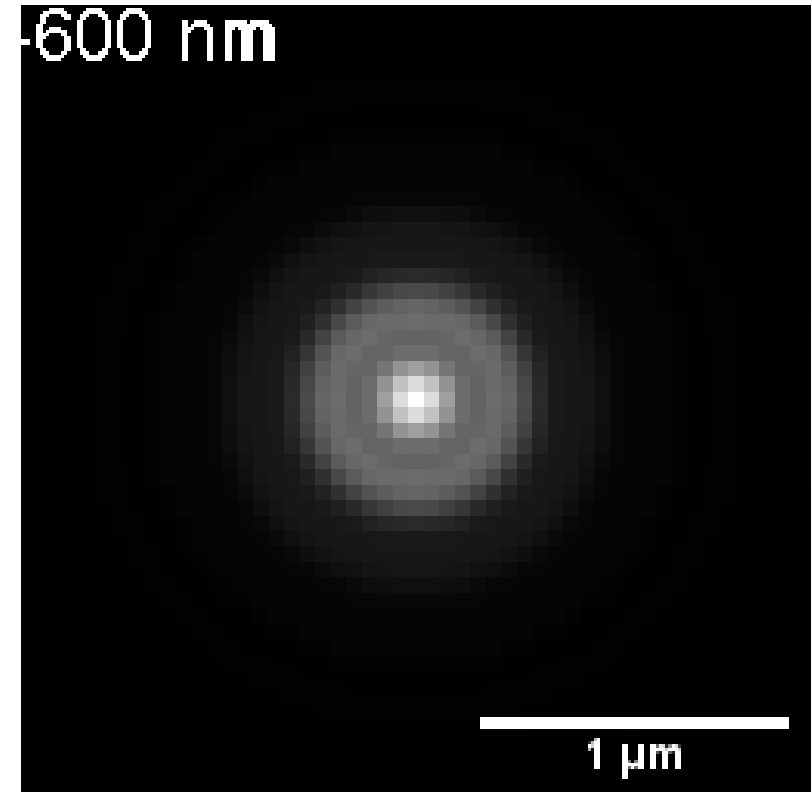
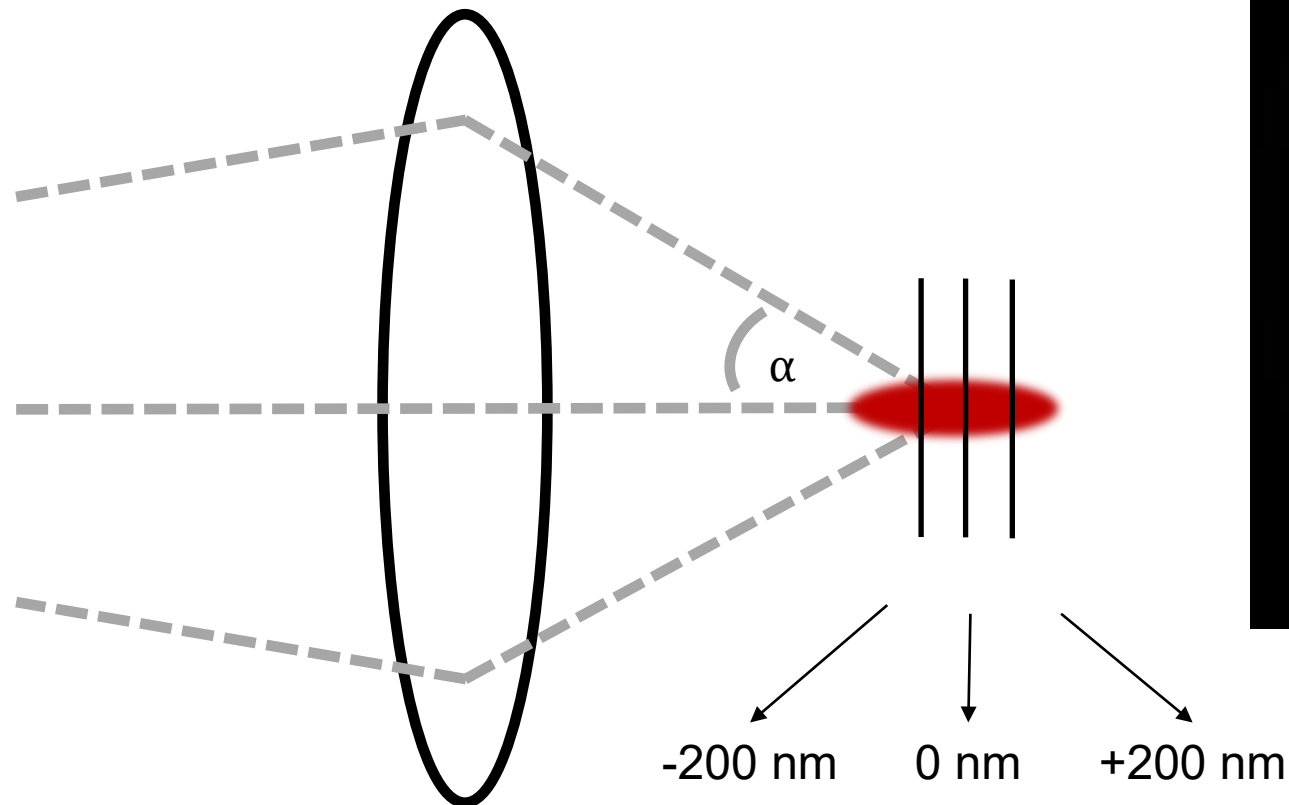
Overview

- Basic principles 2D SMLM 
- Hardware for SMLM 
- Practical considerations: sample preparation, suitable dyes, linkage errors, and buffers 
- Processing, quantification, and interpretation of SMLM data 
- 3D SMLM
- Summary
- Extra: New directions in SMLM
- Extra: SRM as a multidimensional challenge

3D SMLM

Can we localize SM in the axial direction?

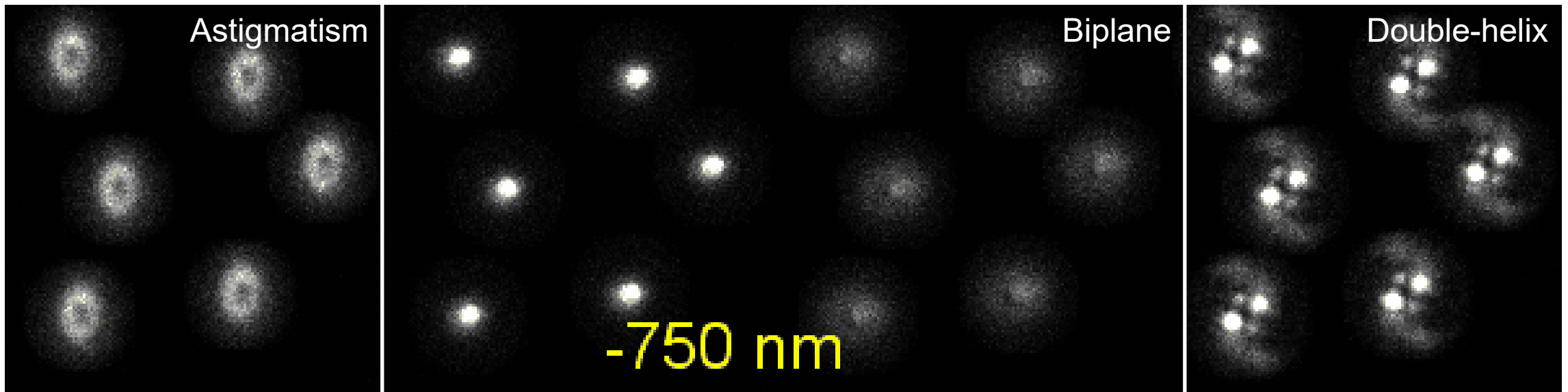
A microscope's PSF is symmetric in the axial direction, which complicates single molecules' localization along the axial axes.



Simulated PSF

Decoding the axial information

Breaking the symmetry of the PSF enables us to decode axial information.

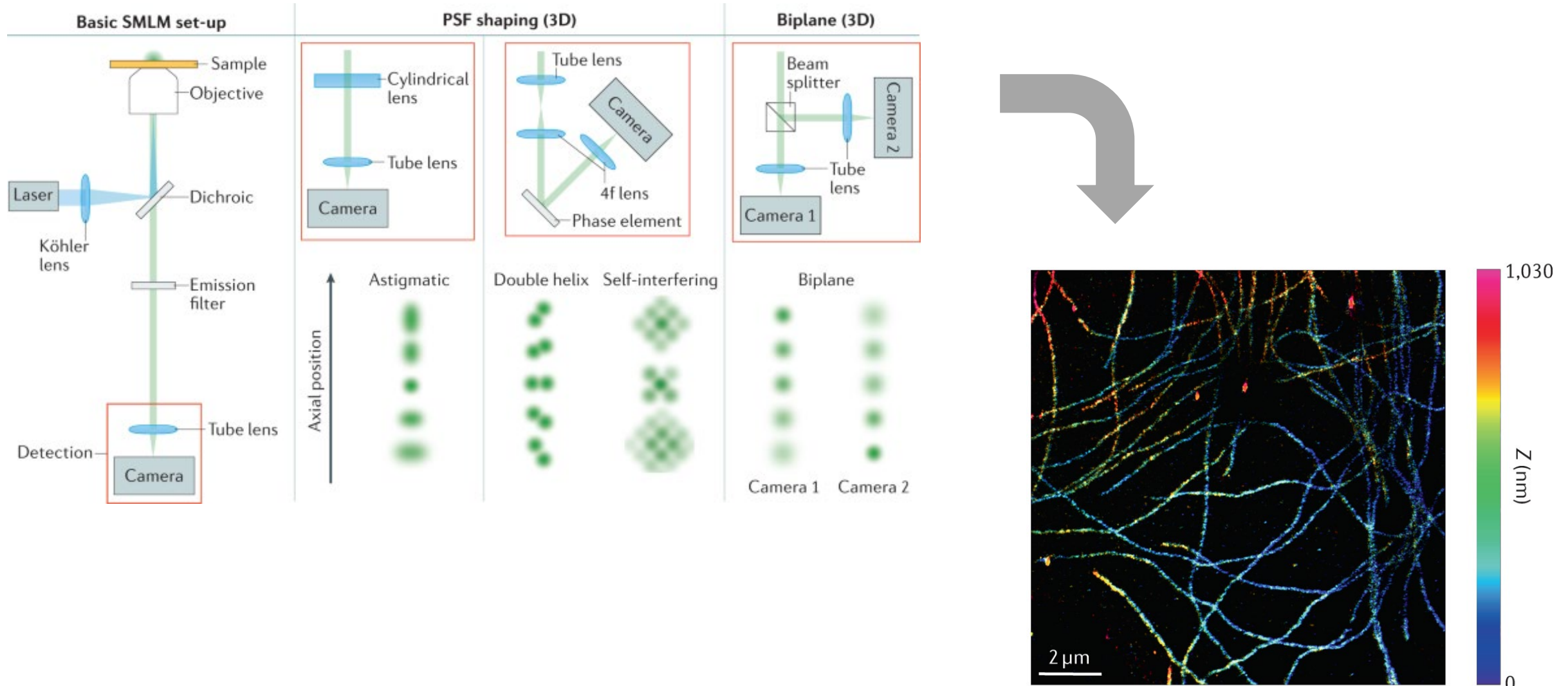


Cylindrical lens in
detection path

Emitted light detected onto two cameras (or two
halves of one camera) defocused relative to one
another

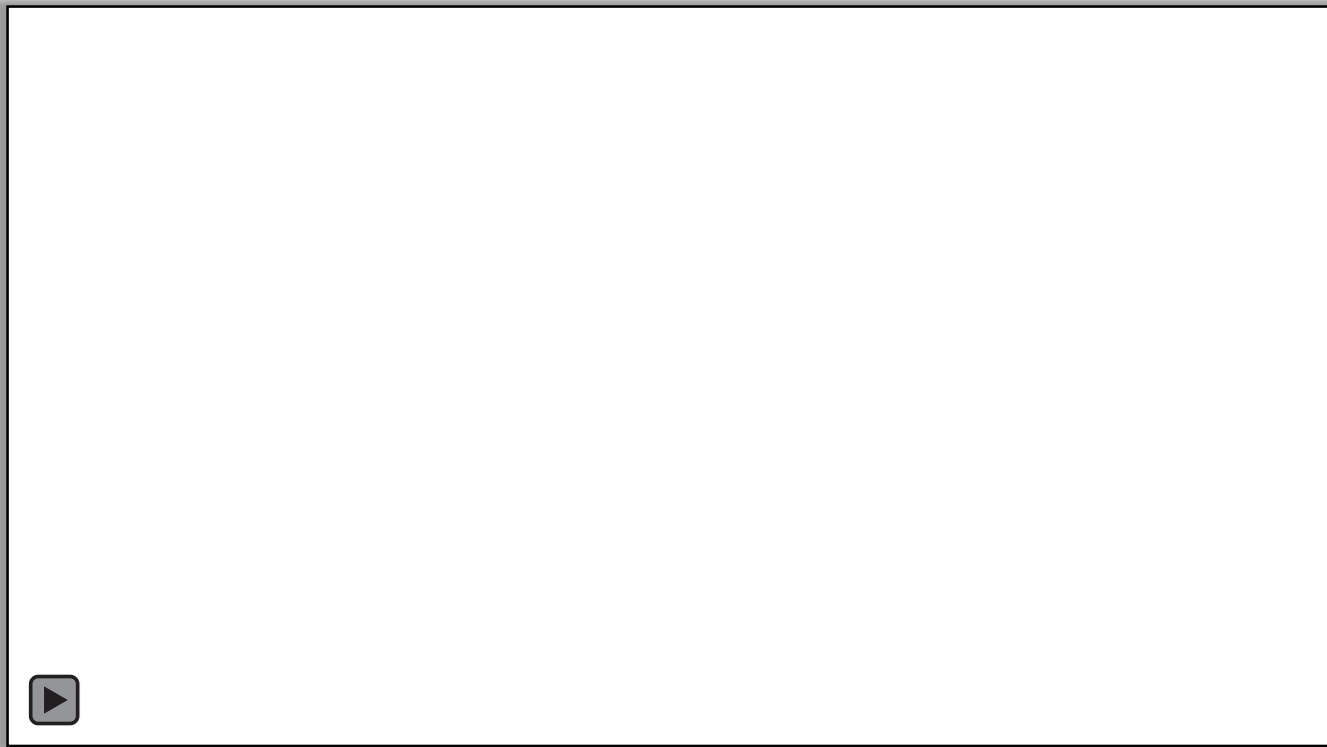
Spatial light modulator /
phase mask in
detection path

Decoding the axial information

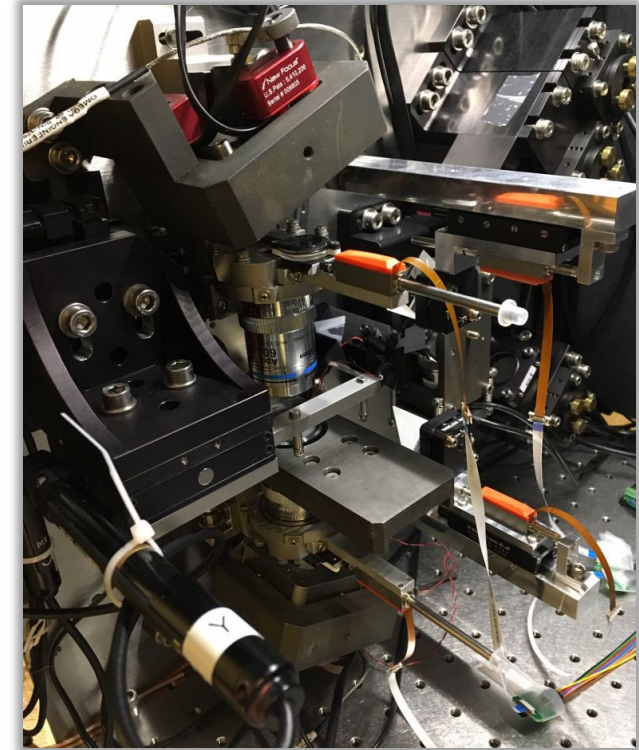


Decoding the axial information

Breaking the symmetry of the PSF enables us to decode axial information.








Resolution: 10-20 nm in all three dimensions



iPALM

Overview

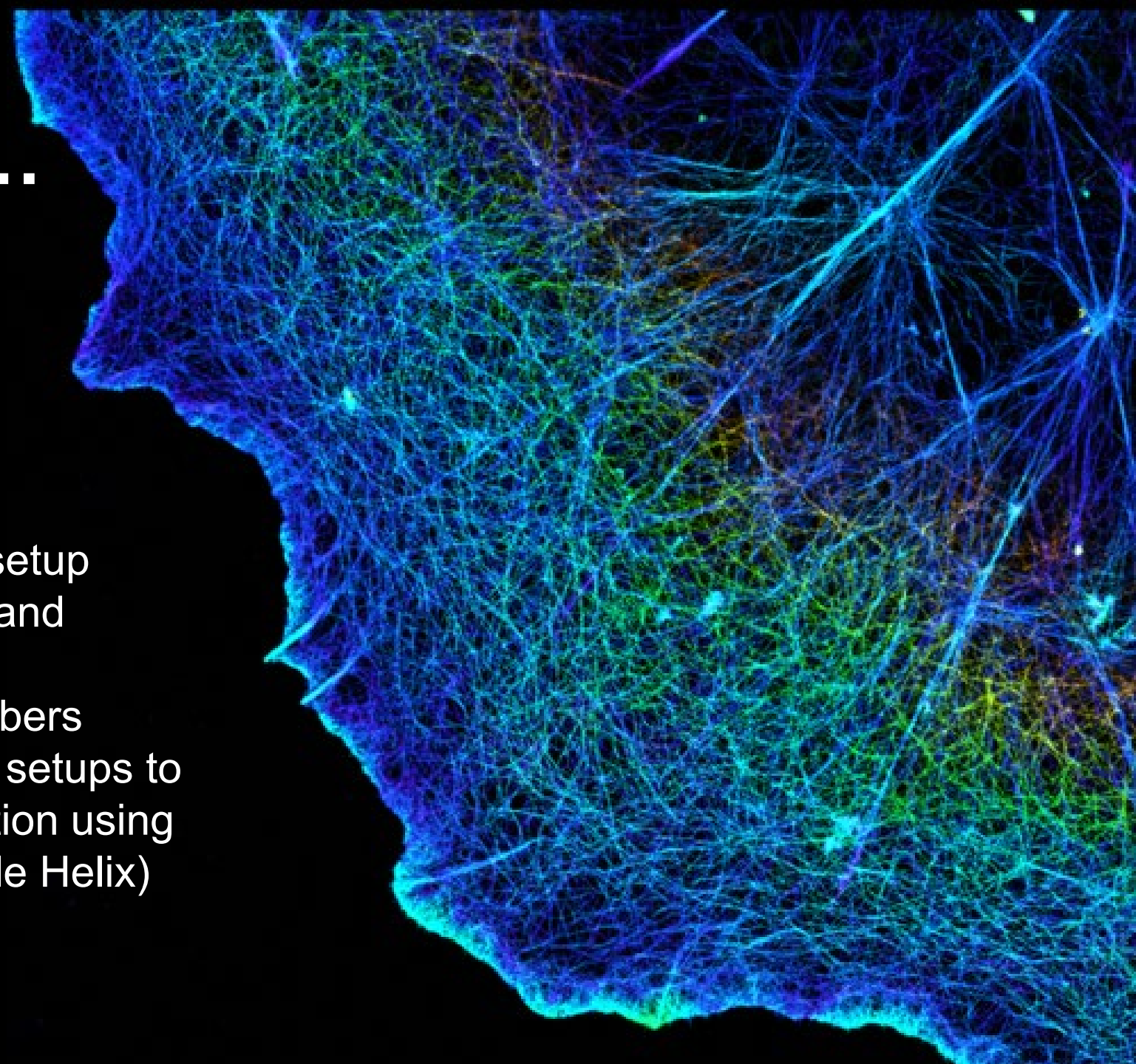
- Basic principles 2D SMLM 
- Hardware for SMLM 
- Practical considerations: sample preparation, suitable dyes, linkage errors, and buffers 
- Processing, quantification, and interpretation of SMLM data 
- 3D SMLM 
- Summary
- Extra: New directions in SMLM
- Extra: SRM as a multidimensional challenge

Summary

Let's wrap it up...

Merits

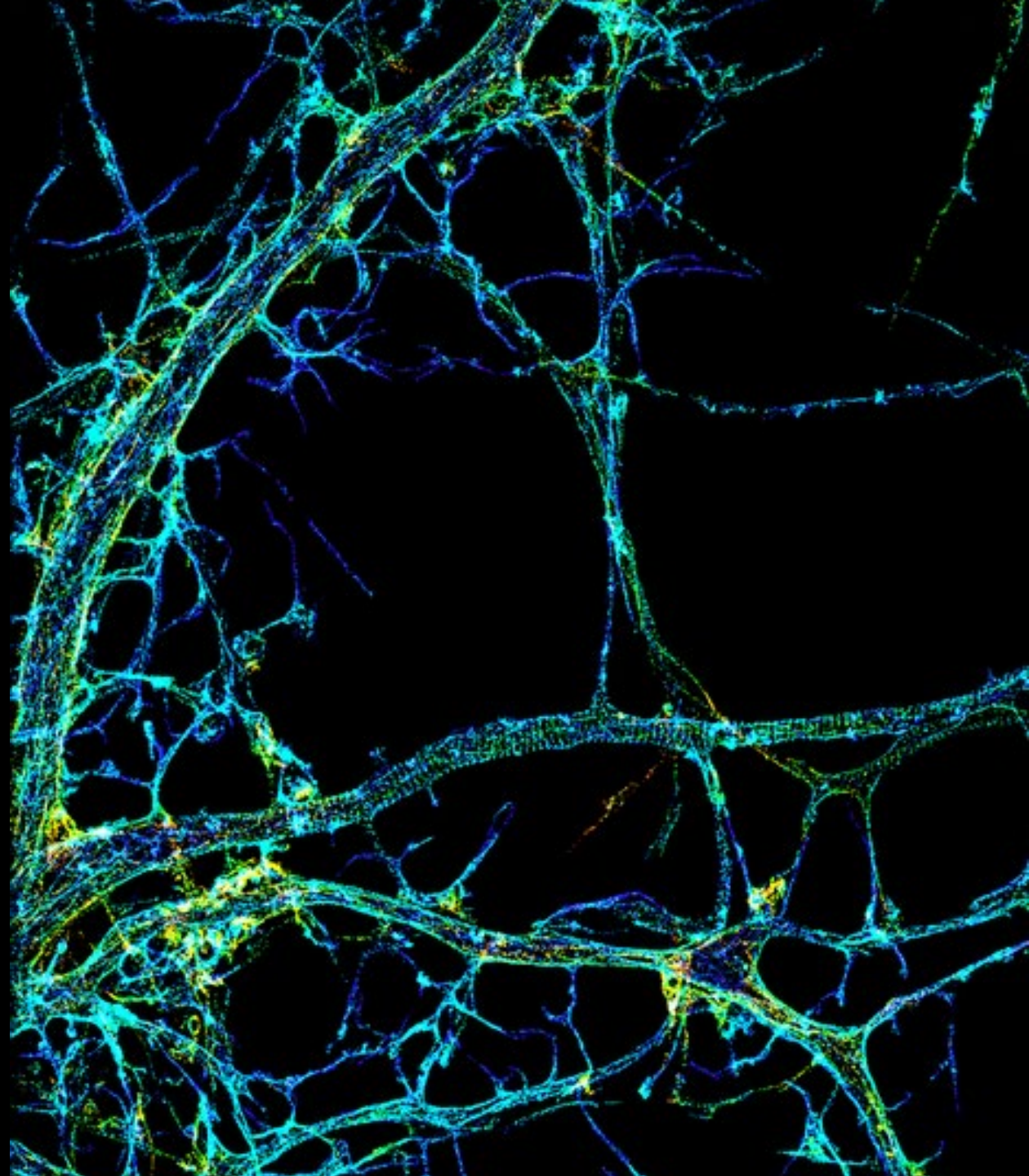
- Very high resolution
- Single molecule detection
- Relative simple microscope setup
- Can be combined with TIRF and inclined illumination (HILO)
- Quantification of protein numbers
- Upgrade solution for exciting setups to enable extended 3D localization using PSF engineering (e.g., Double Helix)









Let's wrap it up...

Disadvantages

- Special buffers/probes required
- Not for thick samples ($< 10 \mu\text{m}$)
- Slow acquisition
- Limited 3D (no sectioning)
- Advanced post-processing needed
- Prone to reconstruction artifacts
- Structural resolution labeling density-dependent



Overview

- Basic principles 2D SMLM 
- Hardware for SMLM 
- Practical considerations: sample preparation, suitable dyes, linkage errors, and buffers 
- Processing, quantification, and interpretation of SMLM data 
- 3D SMLM 
- Summary 
- Extra: New directions in SMLM
- Extra: SRM as a multidimensional challenge

Thank you! Questions?

Ulrike Boehm, Ph.D.

ulrike.boehm@zeiss.com

Twitter: @ulrike_boehm

Opt to Work at ZEISS

Job openings and applications

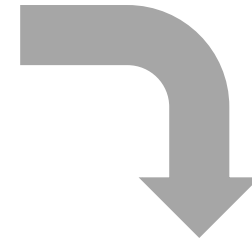
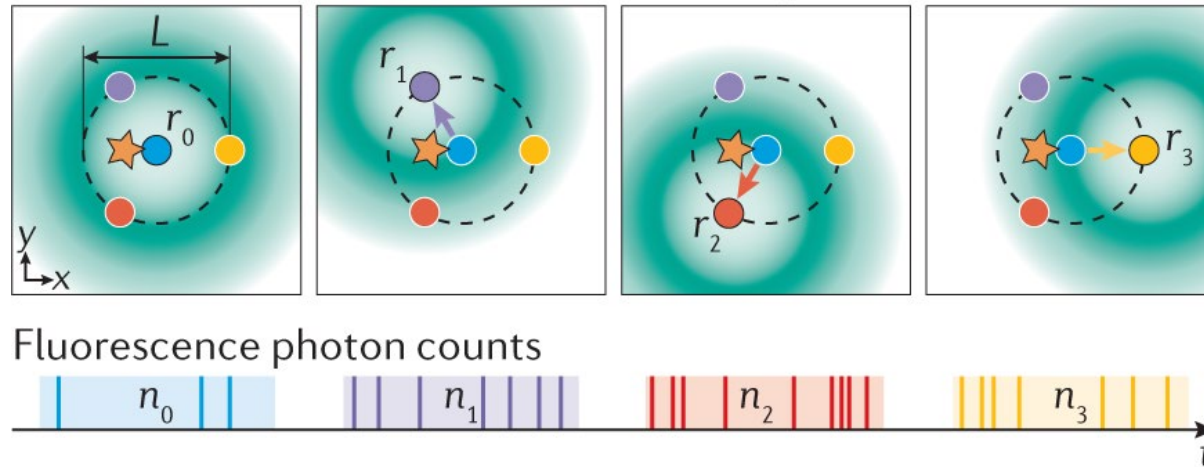
<https://www.zeiss.com/corporate/int/careers/job-openings-and-applications.html>

Photo: Martin Duckek

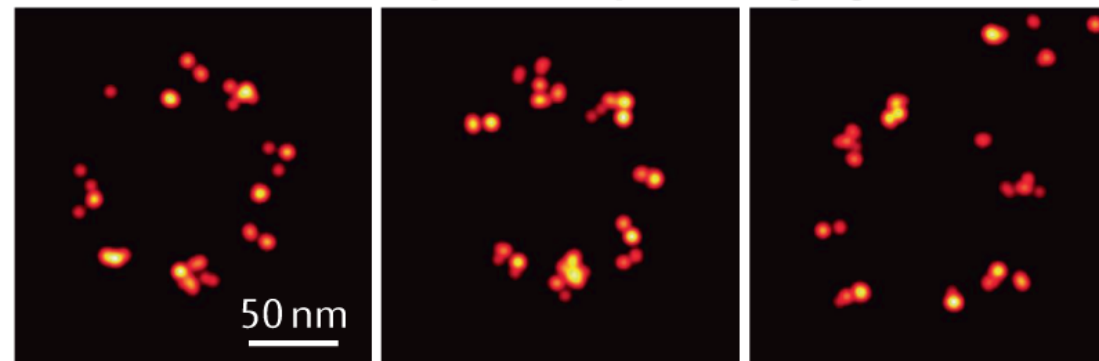
New dimensions in SMLM

MINFLUX emitter localization concept

a MINFLUX emitter localization concept

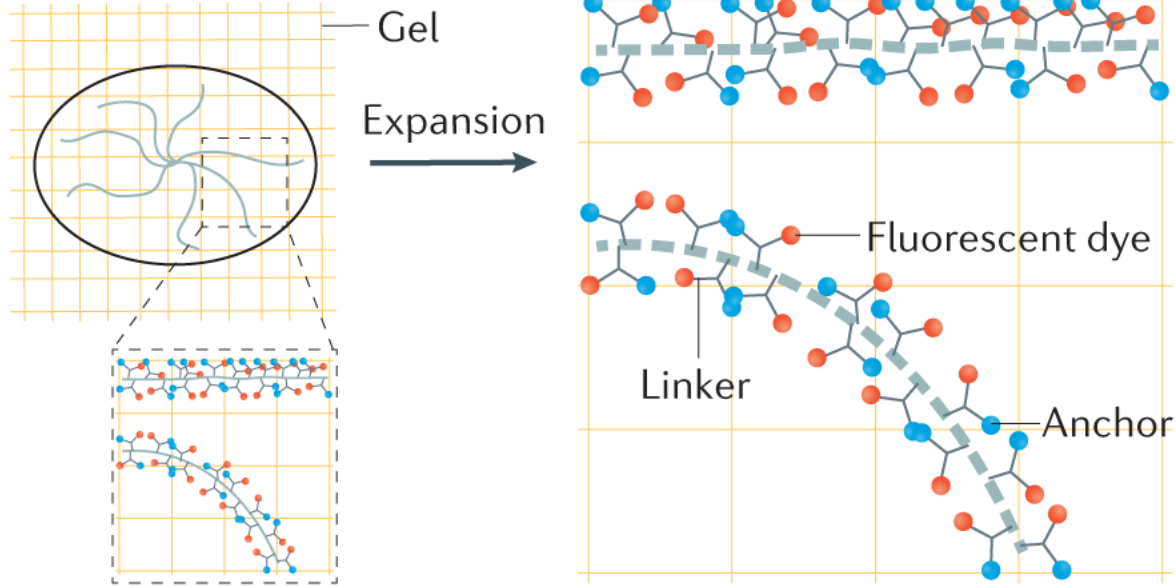


b MINFLUX nuclear pore complex imaging

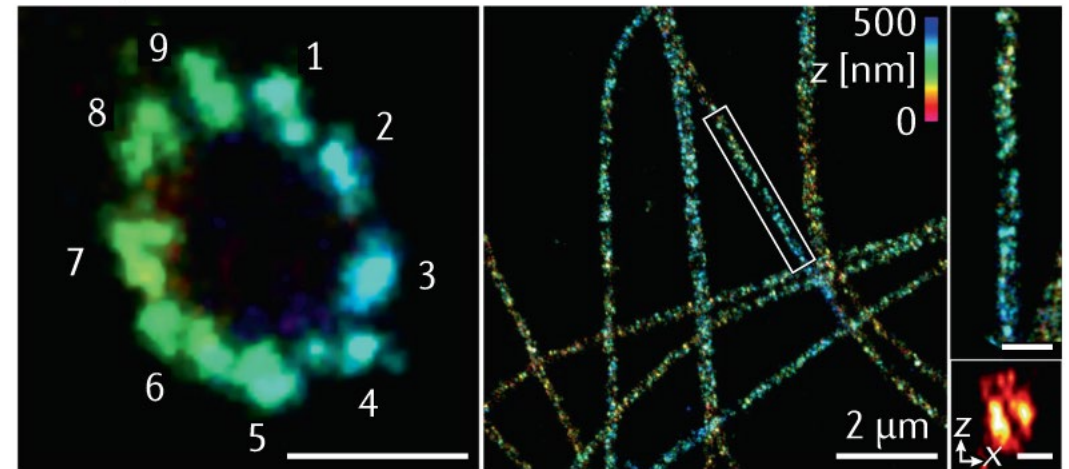


Expansion SMLM

c Expansion microscopy

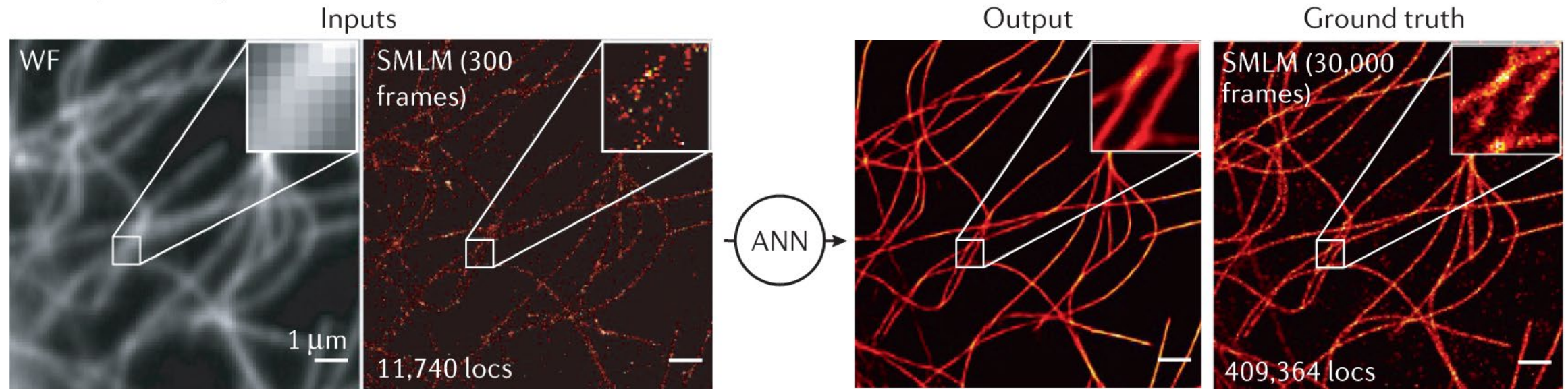


d Expansion SMLM



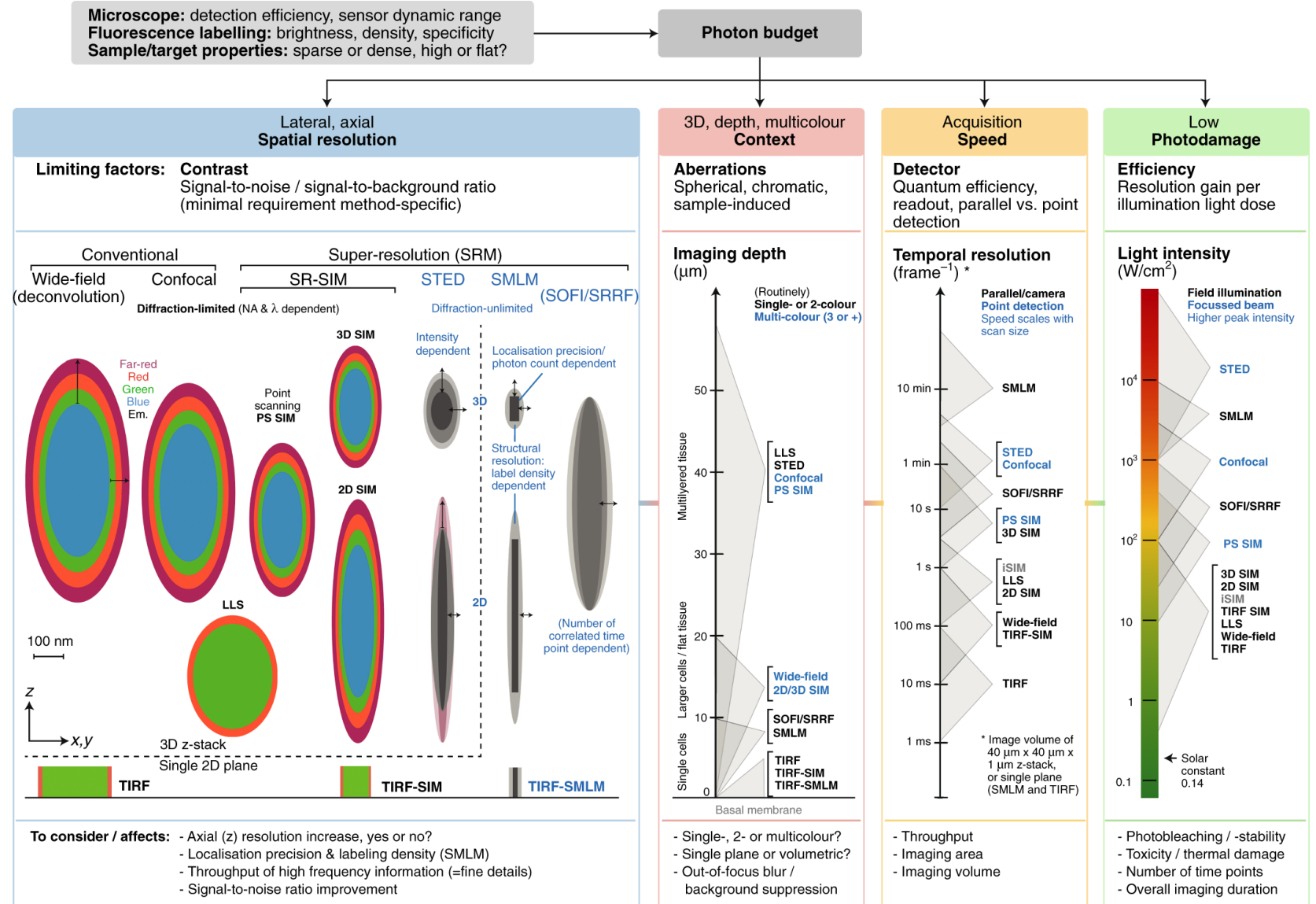
Deep learning-accelerated SMLM

e Deep learning-accelerated SMLM

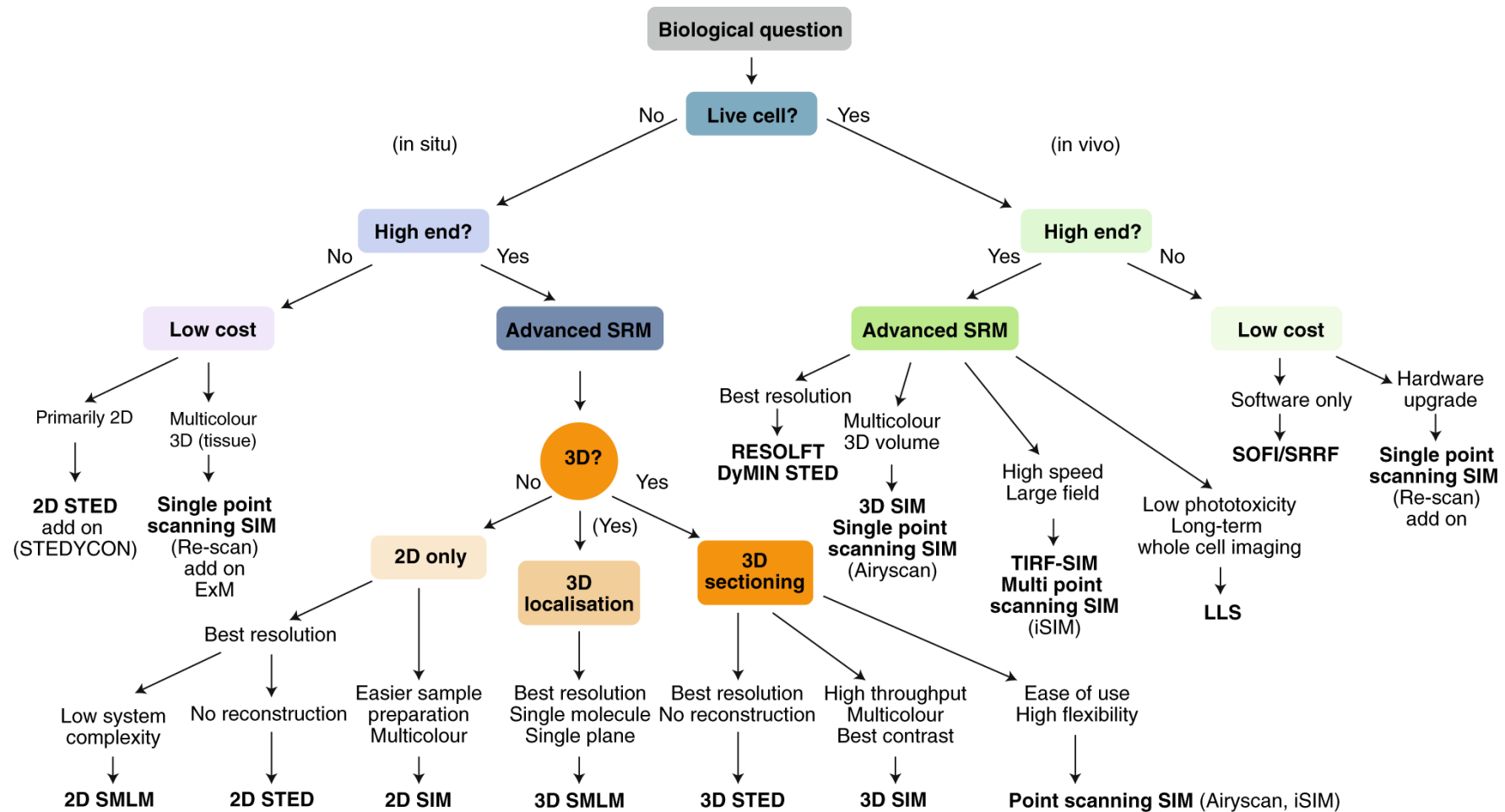


SRM as a multidimensional challenge

Inherent trade-offs in SRM



Decision tree for selecting SRM techniques



Appendix

Switching buffers

Buffer class	Buffer base	Compounds	Organic dyes used in switching buffer / description
Reducer - O₂	PBS/TRIS pH 7.4 - 9 - O ₂	10 - 100 mM MEA	AF 750 [96], CF 680 [63], CF 647 [63], AF 647 and Cy5 [10], CF 568 [63], AF 532 [106], ATTO 520 [103]
		0.5 - 1% BME	AF 750 [112], CF 680 [98], Cy5 readout pairs [9, 58], AF 647 [92]
		10 - 100 mM GSH	AF 647 [106], TMR [106]
Reducer only	PBS/TRIS pH 7.4 - 9	10 - 100 mM MEA	AF 647 [54], ATTO 655 [100], AF 568 [54], ATTO 520 [111], AF 532 [105], AF 488 [111]
		0.5 - 1% BME	ATTO 655 [100]
		50 μM AA	ATTO 655 [169]
		10 - 100 mM GSH	ATTO 655 [52], ATTO 520 [52]
		50 mM TCEP + 2 mM COT	AF 750 [97], AF 647 [97]
Oxygen removal (- O₂)	PBS/TRIS pH 7.4 - 9	GLOX*	AF 568 [121], ATTO 520 [121], AF 488 [121]
		PCD/PCA*	
		POC*	
		100 mM MEA + 1 μM MB	Cy5 [170]

Switching buffers

Switching ROXS reducer and oxidizer - O ₂	PBS/TRIS pH 7.4 - 9	500 μM AA + 25 μM MV	ATTO 655 [171]
	- O ₂	1 mM AA + 1 mM MV + 25 mM TCEP, pH 9	AF 750 [172], AF 647 [172], Cy5 [172]
Switching mount	Vectashield	20% Vectashield + 80% (95% glycerol 50 mM TRIS)	AF 647 [110], CF 647 [110]
	Mowiol	0.5% Mowiol + 50 mM DTT	SiR [101]
	Resin	100% dehydration + EM resin embedding	
	PVA	1% in PBS, spin coat	Oregon Green [41], AF 488 [41]
Live-cell media	DMEM, modified to not contain phenol red	None	SiR [102], TMR [55, 102]
		100 mM GSH + GLOX	AF 647 [106], TMR [106]
		25 mM TCEP	AF 647 [172], Cy5 [172]

Multicolor SMLM

	Name	Dual color combinations	Triple color combinations
Fluorescent proteins	mEos2 (G)	AF 647 [90-92], ATTO 655 [53], Caged SiRhQ [57], Dronpa [56], psCFP2 [56]	eYFP + NileRed [93], PAmKate + Dendra2 [60] PAmKate + PAmCherry1 [60] PAmKate + PAmCherry1 [60], PAtagRFP + ATTO 655 [95]
	mEos2 (R)		
	PAmCherry1	paGFP [59]	
	Dendra2 (G)		
	Dendra2 (R)		
	paGFP	PAmCherry [59]	

	Name	Dual color combinations	Triple color combinations
Organic dyes	Alexa Fluor 750	AF 647 [97]	
	CF 680	AF 647 (#) [62, 98, 99]	CF 660C + DyLight 650 + Dy 634 (#) [62], CF 647 + CF 568 (#) [63]
	ATTO 655 (§)	ATTO 520 [52], mEos2 [53]	PAtagRFP + paGFP [95]
	SiR (§)	mEos2 [57]	TMR + paGFP [102]
	Alexa Fluor 647	ATTO 520 [103], AF 532 [104, 105], ATTO 532 [54], AF 546 [54], AF 568 [54], TMR [106], mEos2 [90-92], AF 488 [91], psCFP2 [56], mMaple [99], ATTO 488 [107], CF 680 (#) [62,98, 99], AF 700 (#) [61], AF 750 (#) [97], Dy678 (#) [108], Dronpa [109]	AF 568 + ATTO 488 [107]
	CF 647		CF 680 (#) + CF 568 [63]
	Cy5		
	Alexa Fluor 568	AF 647 [54]	AF 647 + ATTO 488 [107]
	CF 568		CF 680 + CF 647 [63]
	TMR (§)	AF 647 [106], Citrine [55]	SiR + paGFP [102]
	Alexa Fluor 532	AF 647 [104, 105]	
	ATTO 520	AF 647 [103], ATTO 655 [52]	
	Alexa Fluor 488 (§)	AF 647 [91]	AF 647 + AF 568 [107], Cy3 + ATTO 532 [55], Rhodamine 3C + AF 514 [55]
Cy5/AF 647 readout dye pairs	Reporter: AF 750 [112] Activator: Cy3 + AF 405 [112]	Reporters: Cy7 + Cy5.5 [58] Activators: Cy3 + Cy2 + AF 405 [58]	